Virus-host metabolic interactions: using metabolomics to probe oxidative stress, inflammation and systemic immunity

Schoeman, J.C.

Chapter 3

Metabolomics profiling of the free and total oxidised lipids in urine by LC-MS/MS: application in patients with rheumatoid arthritis

Johannes C. Schoeman*, Junzeng. Fu*, Amy C. Harms, Herman A. van Wietmarschen, Rob J. Vreeken, Ruud Berger, Bart V.J. Cuppen, Floris P.J.G. Lafeber, Jan van der Greef, and Thomas Hankemeier.

Analytical Bioanalytical chemistry (2016) – 408(23):6307-19

* Both authors equally contributed to the manuscript

Abstract

Oxidised lipids, covering enzymatic and auto-oxidation synthesised mediators, are important signalling metabolites in inflammation while also providing a readout for oxidative stress, both of which are prominent physiological processes in a plethora of diseases. Excretion of these metabolites via urine are enhanced through the phase-II conjugation with glucuronic acid, resulting in increased hydrophilicity of these lipid mediators. Here we developed a bovine liver-β-glucuronidase hydrolysing sample preparation method, using liquid chromatography coupled to tandem mass spectrometry to analyse the total urinary oxidised lipid profile including the prostaglandins, isoprostanes, dihydroxy-fatty acids, hydroxy-fatty acids, and the nitro-fatty acids. Our method detected more than 70 oxidised lipids biosynthesised from two non-enzymatic and three enzymatic pathways in urine samples. The total oxidised lipids profiling method was developed and validated for human urine, and was demonstrated for urine samples from patients with rheumatoid arthritis. Pro-inflammatory mediators $PGF_{2\alpha}$, $PGF_{3\alpha}$, and oxidative stress markers $iPF_{2\alpha}IV$, 11-HETE and 14-HDoHE were positively associated with improvement of disease activity score. Furthermore, the anti-inflammatory nitro-fatty acids were negatively associated with baseline disease activity. In conclusion, the developed methodology expands the current metabolic profiling of oxidised lipids in urine, and its application will enhance our understanding of the role these bioactive metabolites play in health and disease.

Background

Oxidised lipids are important signalling mediators in health and disease, capable of providing quantitative readouts relating to inflammatory and oxidative stress status. The *de novo* synthesis of oxidised lipids can be broadly divided into enzymatic and auto-oxidation pathways. The auto-oxidation pathway of oxidised lipids is interlinked with reactive oxygen species (ROS) or reactive nitrogen species (RNS), leading to the peroxidation of fatty acids in membrane bound phospholipids and producing the isoprostanes (IsoPs) [1,2] or nitro-fatty acids (NO_2-FAs) [3]. The lipid peroxidation readout from IsoPs are considered the golden standard for measuring oxidative stress in biological systems [4,5]. Interestingly, NO_2-FAs potentiate diverse anti-inflammatory signalling actions regarded as beneficial within health and disease [3]. These peroxidised lipids impair membrane and organelle integrity and are subsequently excreted from the cell into systemic circulation via cellular repair mechanisms [1].

The enzymatic routes include: i. Cyclooxygenase-I/II/III (COX-I/II/III), synthesising the prostaglandins (PGs), ii. 5/12/15- Lipoxygenase (5/12/15-LOX), synthesising leukotrienes, lipoxins and hydroxyl-fatty acids and lastly iii. Cytochrome P450 (CYP450) responsible for the synthesis of epoxy-fatty acids and dihydroxy-fatty acids [6]. These enzymatically oxidised lipids are synthesised locally from essential free fatty acids and act as signalling mediators in immune modulation and inflammatory responses [6–9]. Due to the potent biological signalling activity of enzymatically oxidised lipids, the active mediators are short-lived in systemic circulation where they are actively metabolised prior to excretion [10]. Thus, taking serum and/or plasma as a representative snapshot of the systemic circulation might not be the most suitable approach to study the oxidised lipid profile. Urine, on the other hand, is a non-invasive bio-fluid, which contains the collected excreted downstream metabolic products. These downstream metabolites provide an enriched systemic readout and are indicative of the presence of the active upstream mediators.

Urine does present some sample specific complications for analysis, such as rather large variations in metabolite concentration, limited solubilities of apolar metabolites and conjugation of some metabolites. These complexities are even more prominent during the analyses of lipid-like metabolites in urine. Due to the partial hydrophobic nature, oxidised lipids are often conjugated to increase their hydrophilicity, mainly by phase-II metabolism located in the liver [11]. Phase II metabolism comprises different enzymatic conjugation reactions, with oxidised lipids most commonly conjugated with glucuronic acid (GlcA) via UDP-glucuronosyltransferases [12–18]. Effectively the oxidised lipids can be excreted in different forms via urine: the unconjugated (free) and the conjugated species [15,17]. The GlcA-conjugated oxidised lipids represent a more hydrophilic form of the metabolites.

Robust metabolic profiling of urinary oxidised lipids has been reported using either gas- or liquid chromatography coupled to mass spectrometry [4,19–27]. However, these methods either detected metabolites in their free form (neglecting the conjugated forms) or focused on a subset of IsoPs and/or PGs. These methodologies lack the broad scope of compounds necessary for a more thorough understanding of disease pathology. Two recent methods reporting on the total (free + conjugated) IsoPs and PGs levels showed increasing urinary metabolite concentrations ranging from 36% to 100% [15,28], indicating the significant

increases when measuring the total concentration, but these methods excluded the LOX and CYP450 oxidised lipid metabolites. Therefore, it is necessary to develop a method able to measure the total urinary oxidised lipids covering the three enzymatic synthesis routes as well as the auto-oxidation metabolites, broadening its biological range.

In the present study we developed and validated robust methods for measuring both the free and total levels of oxidised lipids in human urine samples, covering the PGs, IsoPs, hydroxyl-fatty acids, epoxy fatty acids, leukotrienes, lipoxins and NO_2-FAs. To measure the total oxidised urinary profile, we investigated the suitability of three different ß-glucuronidase enzymes derived from *Helix pomatia*, *Escherichia coli*, and bovine liver. We evaluated these by determining the increase in free metabolites, metabolite stability and enzyme blank effect. Bovine liver derived ß-glucuronidase was chosen as the preferred hydrolysing agent and was used in the total oxidised lipid method and validated concurrently with the free oxidised lipid method. Furthermore, we evaluated the benefit of total level oxidised lipids analyses in urine of rheumatoid arthritis patients. The methodology we established covers a broad scope of oxidised lipid, which enables further investigation of the function and mechanism of these lipids in both health and disease.

Methods

Chemicals and reagents

Ultra-performance liquid chromatography (UPLC)-grade acetonitrile, isopropanol, methanol, ethyl acetate, and purified water were purchased from Biosolve B.V. (Valkenswaard, the Netherlands). Acetic acid, ammonium hydroxide, ammonium acetate, and 2-proponal were acquired from Sigma-Aldrich (Zwijndrecht, the Netherlands). Sodium dihydrogen phosphate dihydrate, sodium hydrogen phosphate and sodium acetate were obtained from Merck (Darmstadt, Germany).

β-glucuronidase enzymes

β-glucuronidase (GUS) from (1) *Helix pomatia* (*H. pomatia*) type H-2 (Aqueous solution, ≥ 85000 units/mL), (2) *Escherichia coli* (*E. coli*) IX-A (Lyophilised power, 1000000-5000000 units/g), and (3) Bovine liver B-1 (Solid, ≥1000000 units/g), together with the exogenous substrate of GUS 4-methylumbelliferyl β-D-glucopyranoside (MUG) were purchased from Sigma-Aldrich Corporation (St. Louis, MO, USA).

Standards and internal standard solutions

Standards and deuterated standards were purchased from Cayman Chemicals (Ann Arbor, MI, USA), Bio-mol (Plymouth Meeting, PA, USA), or Larodan (Malmö, Sweden). Standard and deuterated standard solutions were prepared in methanol containing butylated hydroxy-toluene (BHT) (0.2 mg BHT/EDTA), stored at -80°C. Supplementary Table S3.1 lists an overview of the deuterated internal standards (ISTDs) used in this study.

Urine Sample collection

Collection of control urine for method development

Morning urine was obtained from 10 volunteers (5 males and 5 females) age 27 to 32. The urine samples were pooled, mixed and 400 µL were aliquoted into 2 mL Eppendorf tubes and immediately stored at -80°C prior to extraction.

Rheumatoid arthritis Patients

Oxidised lipid profiling was performed on urine samples derived from an observational study– BiOCURA [29]. In BiOCURA, rheumatoid arthritis (RA) patients eligible for biological disease-modifying anti-rheumatic drugs (bDMARDs) were recruited, and urine samples were collected at random times as baseline samples before initiating bDMARD therapy. Clinical parameters and demographic data were also collected at the start of the study as baseline information, including disease activity measured in 28 joints (DAS28), C-reactive protein (CRP), age, sex, BMI, smoking status, alcohol consumption and concomitant DMARDs. The study was approved by the ethics committee of the University Medical Center Utrecht and the institutional review boards of the participating centres. Human material and human data were handled in accordance with the Declaration of Helsinki and written informed consent was obtained from each patient.

Our analysis was restricted to the BiOCURA patients with baseline (before bDMARDs treatment) disease activity score > 2.6 and good or no drug response after 3-month with Etanercept (ETN) or Adalimumab (ADA) based on the EULAR response criteria. EULAR good response is defined as an improvement in DAS28 > 1.2 and a present DAS28 ≤ 3.2, whereas a EULAR non-response is assigned to patients with an improvement of 0.6-1.2 with present DAS28 > 5.1 or patients with an improvement ≤0.6. In the end, 40 subjects (20 good responders, 20 non-responders) with ETN and 40 subjects (20 good responders, 20 non-responders) with ADA were included in the present study. ETN and ADA are TNF-α inhibitors, which is the most widely used category of bDMARDs.

Methodology development for optimising enzymatic hydrolysis

Hydrolysis conditions were optimised for each of the three GUSs following the approach in Fig. S3.1. Parameters included enzyme concentration (1000U, 1500U, 2000U per sample), incubation temperature (37°C, 55°C) and time (2h, 6h, 12h, 24h). The obtained experimental results for the three enzymes were used to determine the optimal hydrolysing conditions.

Enzymatic hydrolysing conditions

Literature was used to guide the selection of the optimal hydrolysing conditions for the three selected candidate enzymes with regards to the used buffer composition and pH [18,30,31]. For both, *H. pomatia* and bovine liver GUS, a 200 mM acetate buffer (pH 4.5) was used for hydrolysis, and for *E. coli* GUS a hydrolysis buffer of 75 mM phosphate buffer (pH 6.8) was used. As a sensitive GUS substrate, MUG was added into each urine sample as a positive control for monitoring GUS activity.

Enzymatic hydrolysis procedure for GlcA-conjugated oxidised lipids

Ice thawed urine samples (400 µL each) were immediately treated with 10 µL antioxidants (0.2 mg BHT/EDTA) and spiked with 20 µL internal standards (ISTDs) and 5 µL MUG solution. Next, 200 µL of the specific enzyme solution in its appropriate buffer was added to the sample, and the mixture was vortexed and incubated. After hydrolysis samples were put on ice prior to oxidised lipid extraction.

Total and free urinary oxidised lipid extraction

For both, total and free oxidised lipids, the extraction was performed by the same ethyl acetate liquid-liquid extraction procedure. For the analyses of the free oxidised lipids, 400 µL urine were spiked with 10 µL antioxidants and 20 µL ISTDs, similar to the description of enzymatic hydrolysed (total) samples in section 2.3.2. Subsequently, 200 µL citric acid/phosphate buffer (pH 3) was added to the total and free urine samples, and oxidised lipids were extracted by adding 1 mL ethyl acetate followed by shaking for 1 min. Samples were centrifuged at 13000 rpm for 10 min (4°C), after which 800 µL upper organic phase was transferred to a new Eppendorf tube. The LLE was repeated for a second time and the collected organic phase was evaporated to dryness in Labconco CentriVap concentrator (Kansas City, MO, USA). The residues were reconstituted with 30 µL solution of 70% methanol solution containing 100 nM 1-cyclohexyluriedo-3-dodecanoic acid (CUDA) as an external quality marker for the analysis. Afterwards, the extracts were centrifuged at 13000 rpm for 5 min (4°C), and transferred to LC autosampler vials.

Lipid chromatography-mass spectrometry analyses (LC-MS/MS)

The complete oxidised lipid target lists and corresponding ISTDs divided per pathway are shown in supplementary Table S3.2-S3.5. The leukotrienes, hydroxyl-fatty acids, epoxy fatty acids and lipoxins were analysed by high performance liquid chromatography (Agilent 1260, San Jose, CA, USA) coupled to a triple quadrupole mass spectrometer (Agilent 6460, San Jose, CA, USA), using an Ascentis® Express column (2.7 µm, 2.1 × 150 mm) as detailed in Strassburg *et al.* [32].

For adequate PG and IsoP isomer resolution, together with sensitive detection of the NO_2-FAs, an optimised chromatographic method was developed in-house. UHPLC-MS/MS analysis was performed using the Shimadzu LCMS-8050 (Shimadzu, Japan) with a Kromasil EternityXT column (1.8 µm, 50 × 2.1 mm) maintained at 40 °C. The method used a three mobile phase setup with: A (H_2O with 5 mM ammonium acetate and 0.0625% ammonium hydroxide), B (methanol with 0.2% ammonium hydroxide) and C (isopropanol with 0.2% ammonium hydroxide), with a flow rate of 0.6 mL/min. The injection volume was 10 µL and all analytes eluted during a 10-minute ternary gradient with a starting percentage composition of 94.5:5:0.5 (A: B: C). A chromatographic gradient is provided in supplementary Fig. S3.2.

The LCMS-8050 consisted of a triple quadrupole mass spectrometer with a heated electrospray ionisation (ESI) source. In negative ion mode, the source parameters were as follows: the heat block temperature was 400 °C, with the heating gas at 250 °C and a flow of 10 L/min. The nebulising and drying gas had a flow rate of 3 L/min and 10 L/min, respectively. The interface voltage was set at 4 kV with a

temperature of 150 °C. The conversion dynode was set at 10 kV and, and desolvation temperature was 250 °C. Analytes were detected in negative MRM mode.

Method validation

The targeted profiling of oxidised lipids has been previously validated for plasma samples and the performance characteristics linearity, intra- and inter-day precision and accuracy were reported [32]. In the present study, we used the same chromatography parameters in term of the columns, mobile phase, gradient, etc. Therefore, the current validation was performed to determine recovery, matrix effect, and precision for the ISTDs for the reported extraction method.

Creatinine analysis

Urine samples of RA patients were collected at a random time of day, therefore the amount of liquids consumed influenced the concentration of the oxidised lipids in the samples. To eliminate this influence, levels of urinary creatinine were used to correct for dilution. Creatinine levels were determined based on a fast creatinine (urinary) assay kit (Item No. 500701, Cayman Chemical Company, Ann Arbor, MI, USA).

Data processing and statistical analyses

Peak determination and peak area integration were performed with Mass Hunter Quantitative Analysis (Agilent, Version B.04.00) and LabSolutions (Shimadzu, Version 5.65). The obtained peak areas of targets were first corrected by appropriate ISTD and creatinine concentrations (mg/dL), then normalised by log transformation. After data pre-processing, categorical principal component analysis (CATPCA, Supplementary methods) [33] and multiple linear regressions (MLR) were applied to explore the relationships between oxidised lipids and clinical parameters. Cytoscape was used to visualise the associations [34]. All statistical analysis was performed using IBM SPSS Statistics 23.0 software (Chicago, IL, USA).

Results

Optimisation for the hydrolysis of IsoPs, PGs and NO_2-FAs

For determining the optimal enzymatic deconjugation procedure for urinary oxidised lipids, three GUSs derived from *H. pomatia*, *E. coli* and bovine liver were investigated. During the method development, critical parameters including enzyme concentrations, hydrolysis temperature and time were optimised. In order to simplify the method optimisation, we focused on the quantification of a pre-selected panel of metabolites to evaluate the method performance, which covers the most studied IsoPs, PGs and NO_2-FAs in human body fluids. The selected panel consisted of: F-series IsoPs (8-iso-$PGF_{2\alpha}$, 8-iso-15(R)-$PGF_{2\alpha}$, and 8-iso-13,14-dihydro-$PGF_{2\alpha}$), F- and E-series PGs ($PGF_{2\alpha}$, 13,14-dihydro-$PGF_{2\alpha}$, PGE_1, and PGE_2) and two NO_2-FAs mediators (NO_2-linoleic acid and NO_2-oleic acid) (see supplementary Table S3.6).

For all three GUSs tested the optimal conditions was 1000 U enzyme/400 µL urine incubated at 37 °C for 2 hours. No increase in metabolite levels were achieved through increasing the hydrolysis time beyond

2h, or from increasing the temperature (data not shown). Choosing the shortest possible hydrolysis time will also increase the throughput of the method. Fig. 3.1A presents the increase (or decrease) of the concentration (as reflected by the increase of the peak area) in the sample after hydrolysis compared to prior to the hydrolysis for a selected panel of compounds. Significant increases were observed for the F-series IsoPs—all three enzymes increased the metabolite levels by more than 50%. Some downstream metabolites, 8-iso-13,14-dihydro-$PGF_{2\alpha}$ and 13,14-dihydro-$PGF_{2\alpha}$, were exclusively detected after GUS hydrolysis (Fig. 3.1B). No significant increase in the E-series PGs compared to the free levels were found after GUS hydrolysis. The NO_2-FAs mediators could not be analysed after hydrolysis due to their extreme temperature and enzymatic lability (see below for further discussion). No significant differences in the hydrolysis efficiency were found between the three GUSs for the pre-selected panel of compounds. Our final choice of the GUS for our protocol was finally made based on encountered blank effects of GUSs and metabolite stability in presence of the GUS (see below).

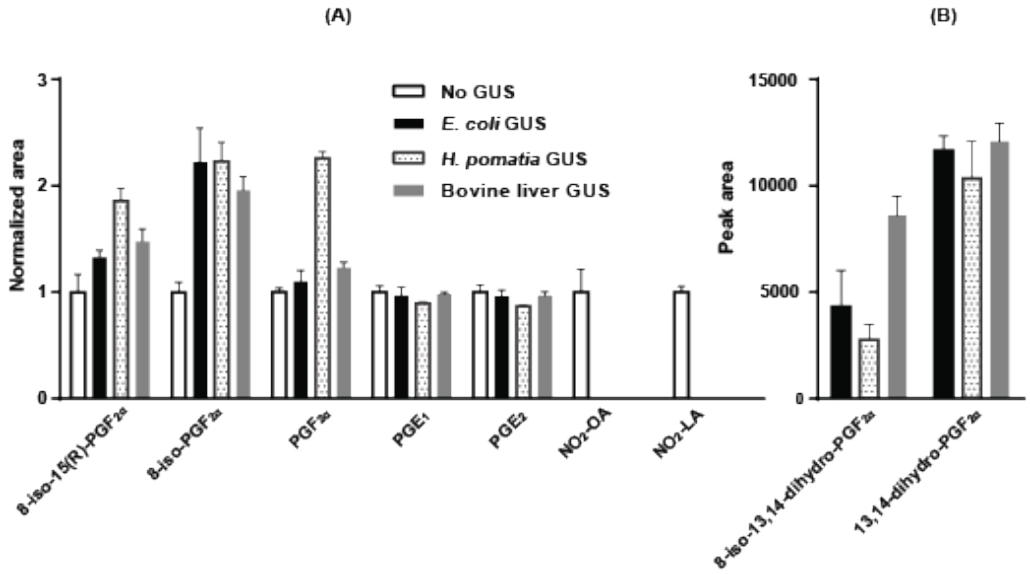

Figure 3.1: Changes in response of the selected panel of compounds in the urine samples after 2h enzymatic hydrolysis (at 37°C with *E. coli*, *H. pomatia*, or bovine liver GUS) compared to non-hydrolysed samples (no GUS). A – Y-axis represents the normalised peak area of a metabolite normalised to the mean area of the corresponding peak in non-hydrolysed urine. B – Y-axis represents the peak area without normalisation since 8-iso-13,14-dihydro-$PGF_{2\alpha}$ and 13,14-dihydro-$PGF_{2\alpha}$ were exclusively detected in GUS hydrolysed urine. Error bars indicate standard deviation.

The enzyme blank effect

We identified an important and so far unreported observation related to an oxidised lipid background present within the three GUSs, especially for *H. pomatia*. Evaluation of the enzyme blank samples, which consisted of water following the GUS hydrolyses sample workup, revealed the presence of an oxidised lipid background. In Fig. 3.2, we show the LC-MS/MS trace for $PGF_{2\alpha}$ and PGE_2 in the non-hydrolysed urine sample, GUS blank samples and procedure blank sample (water sample extracted by LLE, no enzyme added). Fig. 3.2A shows there is no signal for $PGF_{2\alpha}$ in the procedure blank sample while a high level of $PGF_{2\alpha}$ were found especially in the *H. pomatia* GUS blank sample. The levels of $PGF_{2\alpha}$ in *E. coli* and bovine liver GUS samples were lower compared to the high $PGF_{2\alpha}$ background present in *H. pomatia*. Similar observations are made for PGE_2 (Fig. 3.2B). For the selected panel of oxidised lipids, the enzyme blank effect is presented by the area ratio between the blank enzyme sample and the hydrolysed sample at 2h (Area $_{\text{in enzyme blank sample}}$/Area $_{\text{in 2h hydrolysed sample}}$). Inspection of the complete IsoP, PG and NO_2-FA target panel found that *H. pomatia* GUS contained the highest blank effect compared to *E. coli* and bovine liver (see supplementary Table S3.7). Based on this observation *H. pomatia* was not considered as a suitable GUS candidate to measure the total urinary oxidised lipid profile.

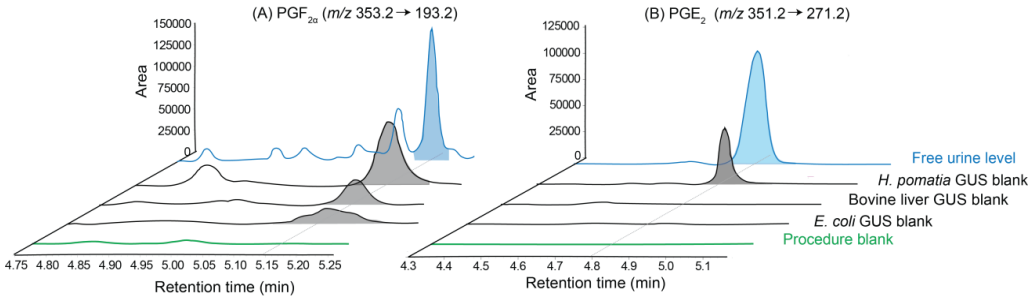

Figure 3.2: The enzymatic oxidised lipid background (enzyme blank effect). LC-MS/MS chromatograms representing the procedure blank (green), followed by the three enzyme blank samples (*E. coli*, bovine liver and *H. pomatia*), and the free urine levels (blue) are overlaid for (A) PGF_{2a} and (B) PGE_2, respectively. *H. pomatia* GUS shows a high oxidised lipid background. Samples were monitored for $PGF_{2\alpha}$ (m/z 353.2 → 193.2) and PGE_2 (m/z 351.2 → 271.2).

Internal standard stability

Beside the enzyme blank effect, the stability of the ISTDs during the 2h incubation at 37°C were investigated as representative for their respective endogenous metabolite classes. The percentage change for the ISTDs treated with the three different enzymes in 2h compared to 0h were determined and are shown in Fig. 3.3. ISTDs representing the F-series PGs and IsoPs were identified as stable at 37°C, over 2h with the addition of an enzyme included, showing less than 10 % change in their levels. However, the E- and D-series

PG ISTDs showed temperature sensitivity, especially PGD_2-d4. Reversely the A series PG ISTD PGA_2-d4 showed increasing concentrations, possibly due to PGD_2-d4 spontaneous dehydration forming PGA_2-d4. The 10-NO_2-Oleic acid d17 (NO_2-FAs ISTD) showed hypersensitivity to hydrolysis conditions (buffer and temperature), showing a 40% decrease in levels within 2h compared to non-hydrolysed sample. Furthermore, the addition of all three enzymes resulted in a more pronounced decrease (70% to 90%), explaining the above mentioned decrease of endogenous NO2-FAs during enzymatic hydrolyses. Overall, the hydrolysis using GUS from *E. coli* showed the largest percentage change for the evaluated ISTDs, suggesting that the 75 mM phosphate buffer (pH 6.8) or *E. coli* GUS affect compound stability. Although, bovine liver GUS showed similar ISTD stability compared to *H. pomatia*, the latter's significant enzyme blank effect led to bovine liver being chosen as our preferred hydrolysing enzyme. Furthermore, bovine liver GUS also resulted in the inclusion of D- and A-series PGs in the target list. Therefore, we chose bovine liver derived GUS hydrolysing at 37°C for 2h as the optimal procedure for analysing the urinary oxidised lipid profile.

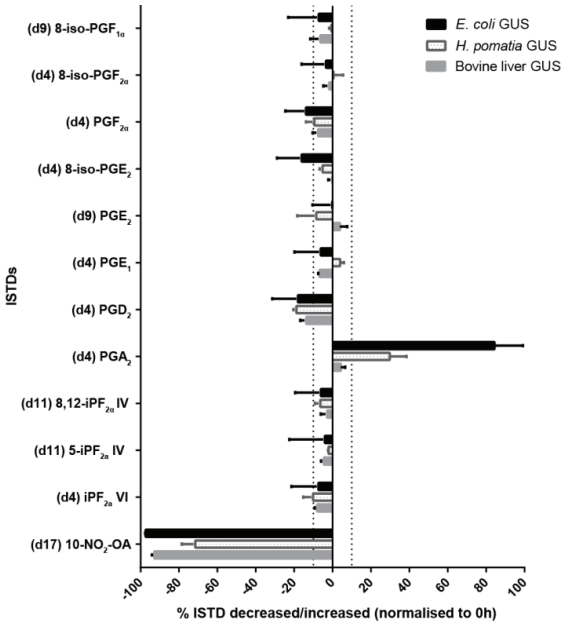

Figure 3.3: The stability of the IsoPs, PGs and NO2-FAs ISTDs during the 2h hydrolyses. The percentage changes of ISTD levels (compare 2h to 0h) were investigated to evaluate the stability of each ISTD. Overall ISTDs with bovine liver GUS hydrolysis indicated the highest degree of stability. The vertical dotted lines indicate 10% change. X-axis indicates percentage changes of ISTD areas between 2h and 0h, (Area $_{2h\text{-}ISTD}$/Area $_{0h\text{-}ISTD}$) × 100%. Error bars indicate standard deviation.

Increasing the metabolite scope

Using the optimised bovine liver hydrolyses method, we investigated the potential to broaden the scope of the measurable oxidised urinary lipid profile. We targeted the metabolites from auto-oxidation, COX, LOX, and CYP450 pathways, and compared the amount of free oxidised lipids (from non-hydrolysed urine) to the total amount of oxidised lipids (from hydrolysed urine). There were 51 metabolites detected in both hydrolysed and non-hydrolysed samples, of which 23 metabolites were significantly increased by hydrolysis. More importantly, 27 additional oxidised lipids were detected exclusively in the total oxidised lipid analysis (Table 3.1). As shown in Table 3.1, we were able to increase the scope of the method by using an enzymatic hydrolysis approach to measure the total urinary oxidised lipid signature, providing a more complete picture for biological interpretation.

Table 3.1: Urinary oxidised lipids measured by bovine liver GUS hydrolysis and non-hydrolysis methods.

	RNS	ROS	COX	LOX	CYP450
Detected in both GUS hydrolysed and non-hydrolysed urine		11-HDoHE*	13,14-dihydro-15-keto-PGE_2*	12S-HEPE	12,13-DiHOME*
		14-HDoHE	15-keto-$PGF_{1\alpha}$	20-carboxy-LTB_4#	12,13-EpOME*
		5-$iPF_{2\alpha}$ VI*	2,3-dinor-11b-$PGF_{2\alpha}$ *	5S,6R-LipoxinA_4	14,15-DiHETrE*
		8,12-$iPF_{2\alpha}$ IV*	2,3-dinor-8-iso-$PGF_{2\alpha}$ *	11-HETE	8,9-DiHETrE*
		8-iso-15(R)-$PGF_{2\alpha}$ *	20-hydroxy-PGE_2#	11-trans-LTD4#	9,10-DiHOME*
		8-iso-15-keto-$PGF_{2\alpha}$ *	Δ12-PGJ_2*	12-HETE	9,10-EpOME*
		8-iso-PGE_1#	Δ17, 6-keto$PGF_{1\alpha}$ *	13-HODE*	
		8-iso-PGE_2	PGA_2	13-KODE	
		8-iso-$PGF_{1\alpha}$	PGD_1#	15-HETE*	
		8-iso-$PGF_{2\alpha}$ *	PGD_2#	5-HETE	
			PGE_1#	9,10,13-TriHOME*	
			PGE_2	9,12,13-TriHOME*	
			PGE_3	9-HODE	
			$PGF_{1\alpha}$	9-HOTrE	
			$PGF_{2\alpha}$*	9-KODE	
			$PGF_{3\alpha}$	LTD_4*	
			PGJ_2#		
			Tetranor-PGEM#		
Detected in GUS hydrolysed urine exclusively		10-HDoHE	13_14-dihydro-$PGF_{2\alpha}$	15S-HETrE	20-HETE
		8-iso-13,14-dihydro-$PGF_{2\alpha}$	13,14-dihydro-15-keto-PGD_2	15-HpETE	12,13-DiHODE
		8-iso-15-keto-$PGF_{2\beta}$	13,14-dihydro-15-keto-$PGF_{2\alpha}$	5S,15S-DiHETE	19,20-DiHDPA
		9-HETE	15-deoxy-Δ-12,14-PGD_2	5S,6S-Lipoxin A_4	11,12-DiHETrE
			15-keto-$PGF_{2\alpha}$	5S-HEPE	11,12-EpETrE
			16-HDoHE	5S-HpETE	14,15-DiHETE
			bicyclo-PGE_2	9-HEPE	17,18-DiHETE
			PGK_2		5,6-DiHETrE
Detected in non-hydrolysed urine exclusively	NO_2-αLA				
	NO_2-LA				
	NO_2-OA				

*: significantly increase with hydrolysis

#: significantly decrease with hydrolysis

Method validation

Validation measurements were performed using pooled urine as a sample matrix. Recovery, matrix effect, and batch-to-batch precision were determined.

Recovery and ion suppression

The performances of the analytical methods (free and total oxidised lipid profiling) with respect to recovery (of the free forms) and ion suppression were validated for those metabolites which were available as deuterium labelled compounds, and which were usually used as ISTDs. For determining recoveries, samples were independently spiked before or spiked after the extraction procedure with ISTDs, and the area ratios between these samples ($Area_{spike\ before}/Area_{spiked\ after}$) were calculated as the recoveries. Fig. 3.4A demonstrates that recoveries are from 85% to 115% for most ISTDs, indicating the effectiveness of both procedures to extract the oxidised metabolome from urine samples. The non-hydrolysed samples (free levels) with a simpler sample handling procedure showed slightly higher recoveries compared to the hydrolysed procedure (total levels) except for the nitro fatty acid ISTD (10-NO_2-oleic acid-d17 as discussed in section 3.1.2).

To determine the ion suppression caused by the presence of compounds of the matrix, ISTDs areas in urine samples spiked after the total and free oxidised lipid extractions were compared to the ISTDs areas in injection solution. Ion suppression values shown in Fig. 3.4B, ranged between 0.5 and 1 for most of the metabolites; values below 1 indicate the presence of ion suppression caused by co-eluting compounds from the urine matrix that were not removed by the sample preparation and that affect the ionisation of those targeted metabolites [35]. Three ISTDs with high ion suppression (lower than 0.5) were PGA_2-d4, 6-ketoPGF_{1}-d4 and TBX_2-d4. However, ion suppression effects are corrected through the deuterated ISTD normalisation ($Area_{\ metabolite}/Area_{\ ISTD}$) as both the metabolite and its corresponding ISTD experience similar ion suppression.

Precision and batch-to-batch effect

To be able to reproducibly and accurately report the oxidised lipid metabolome from patient urine samples, it is important to estimate the analytical variation. Therefore, the intra-batch precision and inter-batch variability were assessed for all endogenous oxidised lipids. Precision is dependent on extraction reproducibility, injection variation and detector stability, while the inter-batch variability is influenced by the robustness of the chromatography and instrument stability across different measurement days (n=3).

In supplementary Fig. S3.3A, the precision (intra-batch RSD) and in Fig. S3.3B the batch-to-batch effect (inter-batch RSD) of endogenous metabolites obtained from hydrolysed/non-hydrolysed urine samples are shown. Investigating the precision for the non-hydrolysed procedure showed that 59 % of metabolites had the RSD < 15%, with a further 25% of metabolites having a RSD between 15% to 30%. The hydrolysed procedure showed improved precision with 66% of metabolites having the RSD < 15%, and 29% of metabolites having a RSD between 15% to 30%. The increased precision observed in the hydrolysed procedure can be attributed to increased metabolites concentrations leading to more accurate detection, while the higher variation in the non-hydrolysed procedure was predominantly driven by low abundant compounds.

Both procedures performed equally well in batch to batch effects, indicative of a stable and reproducible LC-MS analyses across three measurement days.

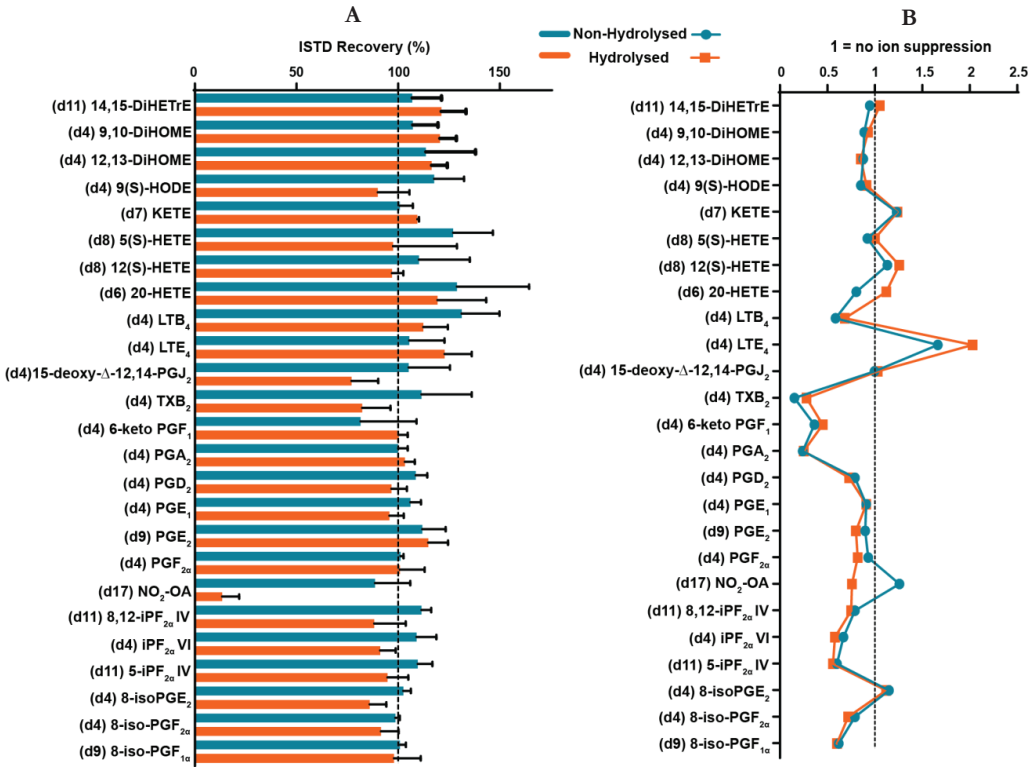

Figure 3.4: Performance characteristics of sample preparation. Deuterium labelled ISTDs were evaluated for (A) recovery and (B) ion suppression; values below 1 indicate presence of ion suppression (B).

Application

Subjects

For the present study, baseline urine samples from RA patients who were treated with TNF-α inhibitors (ETN or ADA) were selected based on good response or non-response after three months of therapy. The baseline characteristics of 80 patients are shown in Table 3.2. Subjects had a mean age of 53.8 years, a median disease duration of 5 years, and had previously taken a mean of two concomitant disease-modifying anti-rheumatic drugs (co-DMARDs). Subjects were mainly female (58 females, 22 males). Good responders had higher baseline DAS28 (4.8 ±0.9 compared with 4.2 ±11, $P = 0.006$) and C-reactive protein

(CRP) levels (8 ± 11 compared with 5 ± 7, $P = 0.04$) compared to the non-responders. There were no significant differences between the other parameters.

Table 3.2: Baseline characteristics of the study subjects (n=80), subdivided according to the therapeutic response at three months.

	All subject (n=80)	Non-response (n=40)	Good response (n=40)	*P* value (good responders vs. non-responders)
Gender, female, n (%)	58 (72.5)	31 (77.5)	27 (67.5)	0.453
Age, mean (SD)	53.8 (11.0)	52.7 (11.3)	55.1 (10.8)	0.461
Disease duration, median (IQR)	5 (8.0)	5 (7.0)	6 (9.0)	1.000
Smoking currently, n (%)	23 (28.7)	12 (30.0)	11 (27.5)	0.805
Alcohol >7 units/week, n (%)	16 (20.3)	5 (12.5)	11 (27.5)	0.099
BMI, mean (SD)	26.9 (5.3)	27.1 (5.0)	26.7 (5.6)	0.874
RF, positive, n (%)	57 (71.3)	26 (65.0)	31 (77.5)	0.323
ACPA, positive, n (%)	57 (71.3)	26 (65.0)	31 (77.5)	0.323
Baseline DAS28, mean (SD)	4.5 (1.0)	4.2 (1.1)	4.8 (0.9)	**0.006**
CRP, median (IQR)	7 (10.0)	5 (8)	8 (11.0)	**0.045**

SD: standard deviation; IQR: interquartile range.

Detection of oxidised lipids in human urine

Applying total and free oxidised lipid profiling to randomly collected urine samples, we are able to detect 67 metabolites in hydrolysed urine samples and 44 in non-hydrolysed urine samples. There were 97% total and 95% free oxidised lipid metabolites measured with a RSD < 30% (see supplementary Table S3.8). Because the total oxidised lipid profiling provides a larger scope of metabolites, we focused on the total urinary oxidised lipid profiles (after hydrolysis), in addition to the free NO_2-FAs levels measured in the analyses without hydrolysis in the subsequent data analyses and interpretation.

Relationships between total oxidised lipids profiling and RA-associated parameters

To investigate the relationship between RA-associated parameters and total oxidised lipid levels, repeated assessments using multiple linear regression (MLR) models were performed on individual metabolite. Confounding factors (age, sex, BMI, smoking status, alcohol consumption, co-DMARDs) and RA-associated parameters (baseline DAS28, CRP and DAS28 improvement) were added into MLR as independent variables, and the oxidised lipid level was set as the dependent variable. RA-associated parameters which were correlated with oxidised lipid levels ($P < 0.10$) were selected (Table S3.9) and are visualised by Cytoscape in Fig. 3.5. CRP showed a positive correlation with 16-HDoHE ($P = 0.027$) and a negative correlation with PGD_3 ($P = 0.026$); DAS 28 showed a positive association with 14,15-DiHETE ($P = 0.036$) and 5S, 6R-LipoxinA4 ($P = 0.005$); DAS28 improvement ($DAS28_{\text{month 0}} - DAS28_{\text{month 3}}$) showed significantly positive association with $PGF_{3\alpha}$ ($P = 0.017$), $PGF_{2\alpha}$ ($P = 0.018$), $iPF_{2\alpha}$ IV ($P = 0.021$), 11, 12-EpETrE ($P = 0.040$), 11-HETE ($P = 0.019$), 14,15-

DiHETrE (P = 0.017) and 14-HDoHE (P = 0.033). Since NO_2-FAs were labile in the hydrolysing procedure, we included the free NO_2-αLA, NO_2-LA and NO_2-OA levels during the MLR. These three metabolites were all negatively associated with baseline DAS28 (P < 0.05).

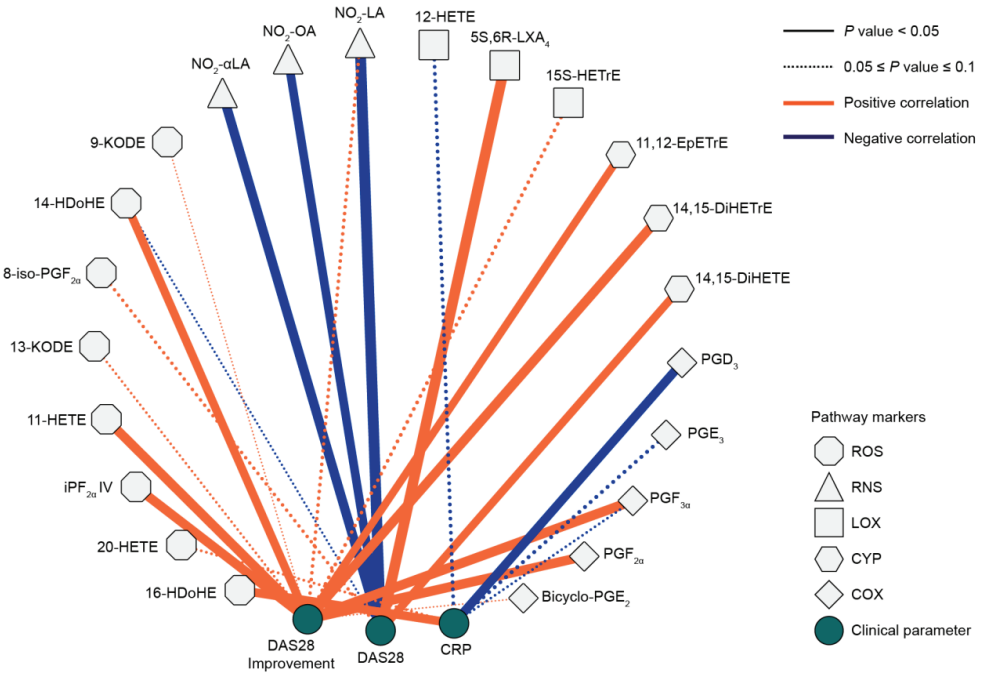

Figure 3.5: Correlations between rheumatoid arthritis-associated clinical parameters and oxidised lipid levels with P < 0.10 based on multiple linear regression analyses.

Discussion

In the present study, we optimised and validated a GUS based hydrolysis method to evaluate the oxidised urinary lipid profile. We demonstrated that the number of measured oxidised lipids were approximately two-fold increased after hydrolysing with bovine liver sourced GUS. Furthermore, we applied the method to urine samples from patients with RA and identified oxidised lipids associated with RA-associated parameters important in determining therapeutic response.

As a non-invasive biological matrix, urine is easily collected and can effectively be used as an oxidised lipids readout. However, urine does present some challenges including dilution effect (morning sample, 24h sample, random sample), glucuronidation of metabolites with low solubility, and a high salt concentration etc. Although some of these challenges can be addressed with proper experimental planning and standardised

sample collection procedures, the choice between analysing free or total levels of oxidised lipids still needs to be addressed. Thus, we developed a robust enzymatic method to hydrolyse the GlcA conjugated oxidised lipids, obtaining the total oxidised lipid profile for urine samples. During the method development, we found an enzyme blank effect in the three candidate enzymes (Table S3.7) which needs to be minimised in order to avoid adding artefacts which could interfere with the biological interpretation of the results.

Several different GUS are available commercially for research purposes, with each enzyme having its own specific characteristics properties relating to substrate affinities and efficiency. Our choice of candidate enzymes was guided by selecting those previously reported in literature [18,30,31]. *H. pomatia* GUS was the most widely used enzyme but had a very prominent blank effect. The oxidised lipid background might be derived from inadequate purifying and cleaning procedures used during enzyme extraction and isolation. While this might not be true for all forms of GUS derived from *H. pomatia*, we decided against the use of *H. pomatia* as the background might influence our biological interpretation of the data.

Comparing the total and free oxidised lipid profiles revealed increased levels, especially in the F-series IsoPs, F-series PGs, hydroxy-fatty acids and dihydroxy-fatty acids, while having minimal effect on E-series PGs in the total oxidised lipid profile. The lack of effect on the E-series PGs could be explained in a study done by Little et al., where they investigated the different human recombinant UDP-glucuronosyltransferases and found that only one isoform UGT2B7 was capable of forming PGE_2 glucuronide [17]. UGT2B7 were exclusively found in the colon, and faeces rather than urine might contain high levels of E-series glucuronide conjugates. The significant increase in LOX and CYP450 metabolites might be due to their increasing hydrophobic nature, with glucuronidation increasing their urinary excretion. Similar to our findings, Prakash *et al.,* reported significant increase in the level of 20-HETE, an CYP450 metabolite in urine treated with β-glucuronidases, and they concluded that CYP450 metabolites are predominantly excreted in conjugated form [13]. Whereas the method reported by Newman *et al.,* needed 4 mL of urine to measure the free CYP450 oxidised lipid metabolites [22]. Using our bovine liver hydrolysis method, we could evaluate the same CYP450 pathway metabolites by using 10 times less urine.

Optimising the extraction and analyses of the anti-inflammatory NO_2-FAs will aid us in studying the field of nitrosative stress. A disappointing finding was our inability to accurately measure the total NO_2-FAs levels, due to their labile nature. Although, we were able to effectively measure the free NO2-αLA, NO_2-LA and NO_2-OA levels in urine. In work published by Salvatore *et al.,* they showed the presence of cysteine-NO_2-FAs conjugates in urine, and used a short chemical ($HgCl_2$) hydrolysis procedure at 37 °C to measure its total levels [36]. Thus, to accurately measure the total NO_2-FAs levels identification of the primary conjugated form needs to be done, followed with optimised chemical hydrolyses.

For the urine samples from RA patients, which were collected at a random time of day, we used the urinary creatinine level for correcting the oxidised lipids for sample dilution. Samples were retrospectively divided into good or no responders to therapy based on EULAR response criteria. However, the subjects could not be separated into non-/good response groups based on their baseline urinary oxidised lipids profile and clinical parameters using categorical principle components analysis (CATPCA, score plot is shown in supplementary Fig. S3.4). After correcting for confounding factors (age, sex, BMI, smoking status, alcohol

consumption, co-DMARDs), the urinary oxidised lipid readout did show associations between inflammation and oxidative stress, and clinical parameters (CRP, 3-month-DAS28 improvement, baseline DAS28). C-Reactive protein is an acute phase inflammatory protein, which showed a positive correlation with 16-HDoHE, a docosahexaenoic acid (DHA) lipid peroxidation metabolite. DHA showed efficacy as an anti-inflammatory treatment when used as a prophylactic treatment in a mouse RA model [37], thus the increased peroxidation of DHA catalysed by ROS reduces the body's anti-inflammatory capacity. Oxidative stress has been identified as an aggravator of damage caused to bone in cartilage in RA [38], [39], so its correlation with CRP underscores this relationship.

DAS28 is the most widely used measurement for assessing the disease activity (swelling and tenderness in 28 joints, the ESR and VAS general health) in RA [40]. In the present study, good responders had higher baseline DAS28 compared to non-responders. Clinically it has been observed that a patient with severe RA has high DAS28 and is more likely to obtain therapeutic response [41]. Veselinovic *et al.,* reported increased levels of RNS in patients with high disease activity in serum [38], while we found in urine that the downstream anti-inflammatory NO_2-FAs correlated negatively with DAS28. This observation could be explained through the complex relationship between RNS species, the beneficial signalling abilities of RNS nitrated lipid metabolites (NO_2-FAs) and the body's anti-oxidant capacity. The positive correlation of DAS28 improvement with strong pro-inflammatory mediators $PGF_{2\alpha}$, $PGF_{3\alpha}$, and oxidative stress markers $iPF_{2\alpha}$, 11-HETE and 14-HDoHE indicate the higher disease burden within these baseline patients. The correlation of DAS28 and its improvement with the anti-inflammatory CYP-450 dihydroxy-fatty acids metabolites and the LOX derived LXA_4 possibly reflects the intact innate anti-inflammatory pathways in these patients still trying to lessen the RA disease burden. The dihydroxy-fatty acids, 14,15-DiHETE, 11, 12-EpETrE, and 14, 15-DiHETrE are able to attenuate pro-inflammatory pathways through activating and signalling via the PPAR-gamma pathway [42]. The urinary oxidised lipid profile of RA patients indicates the complex nature of the disease with oxidative stress and inflammation having an intimate relationship with clinically measured parameters.

Conclusions

In the present study, we thoroughly explored different deglucoronidation methods for urinary oxidised lipids and developed a bovine liver-GUS hydrolysing sample preparation method coupled with LC/MS to analyse the total urinary oxidised lipid profile. With bovine liver GUS hydrolysis, we are able to zoom into the urinary oxidised lipid metabolome, providing a readout for inflammation and oxidative stress. Our method detected more than 70 oxidised lipids in urine samples, biosynthesised from 2 non-enzymatic and 3 enzymatic pathways. The total oxidised lipid profiling method was developed and validated for human urine, and was demonstrated on patients with RA. The urinary oxidised lipid profile of RA patients indicates the complex nature of the disease with oxidative stress and inflammation having an intimate relationship with clinically measured parameters. In conclusion, the hydrolysed method developed here allows specific and sensitive quantitative assessment of more than 70 oxidised lipids, which expands the scope of compounds in urinary metabolic profiling, and may have wider applications in studies elucidating the role of these potent bioactive metabolites in human diseases.

Acknowledgments

The authors express their gratitude to the people from the University Medical Centre Utrecht for providing the samples of BioCURA. The authors thank L. Lamont-de Vries for the help in sample analysis. The China Scholarship Council is also gratefully acknowledged (J. Fu, file number 201206200123). The funding provided by the Virgo consortium for J.C. Schoeman, funded by the Dutch government project number FES0908.

References

1. Montuschi, P., Barnes, P. J. & Roberts, L. J. Isoprostanes: markers and mediators of oxidative stress. *FASEB J.* **18,** 1791–1800 (2004).
2. Milne, G. L., Yin, H., Hardy, K. D., Davies, S. S. & Roberts, L. J. Isoprostane generation and function. *Chem. Rev.* **111,** 5973–5996 (2011).
3. Baker, P. R. S., Schopfer, F. J., O'Donnell, V. B. & Freeman, B. A. Convergence of nitric oxide and lipid signaling: Anti-inflammatory nitro-fatty acids. *Free Radic. Biol. Med.* **46,** 989–1003 (2009).
4. Richelle, M. *et al.* Urinary isoprostane excretion is not confounded by the lipid content of the diet. *FEBS Lett.* **459,** 259–262 (1999).
5. Galano, J.-M., Lee, Y. Y., Durand, T. & Lee, J. C.-Y. Special issue on 'Analytical methods for oxidized biomolecules and antioxidants' The use of isoprostanoids as biomarkers of oxidative damage, and their role in human dietary intervention studies. *Free Radic. Res.* **49,** 583–98 (2015).
6. Buczynski, M. W., Dumlao, D. S. & Dennis, E. A. Thematic Review Series: Proteomics. An integrated omics analysis of eicosanoid biology. *J. Lipid Res.* **50,** 1015–1038 (2009).
7. Stables, M. J. & Gilroy, D. W. Old and new generation lipid mediators in acute inflammation and resolution. *Prog. Lipid Res.* **50,** 35–51 (2011).
8. Smyth, E. M., Grosser, T., Wang, M., Yu, Y. & FitzGerald, G. A. Prostanoids in health and disease. *J. Lipid Res.* **50,** S423–S428 (2009).
9. Serhan, C. N. Novel lipid mediators and resolution mechanisms in acute inflammation: to resolve or not? *Am. J. Pathol.* **177,** 1576–91 (2010).
10. Tai, H. H., Ensor, C. M., Tong, M., Zhou, H. & Yan, F. Prostaglandin catabolizing enzymes. *Prostaglandins Other Lipid Mediat.* **68-69,** 483–493 (2002).
11. Stachulski, A. V & Meng, X. Glucuronides from metabolites to medicines: a survey of the in vivo generation, chemical synthesis and properties of glucuronides. *Nat. Prod. Rep.* **30,** 806–48 (2013).
12. Trontelj, J. Quantification of Glucuronide Metabolites in Biological Matrices by LC-MS/MS. *Tandem Mass Spectrom. - Appl. Princ.* 531–558 (2012). doi:10.5772/30923
13. Prakash, C., Zhang, J. Y., Falck, J. R., Chauhan, K. & Blair, I. A. 20-Hydroxyeicosatetraenoic acid is excreted as a glucuronide conjugate in human urine. *Biochem. Biophys. Res. Commun.* **185,** 728–733 (1992).
14. Schwartz, M. S., Desai, R. B., Bi, S., Miller, A. R. & Matuszewski, B. K. Determination of a prostaglandin D2 antagonist and its acyl glucuronide metabolite in human plasma by high performance liquid chromatography with tandem mass spectrometric detection--a lack of MS/MS selectivity between a glucuronide conjugate and a phase . *J. Chromatogr. B. Analyt. Technol. Biomed. Life Sci.* **837,** 116–24 (2006).

15. Yan, Z., Mas, E., Mori, T. A., Croft, K. D. & Barden, A. E. A significant proportion of F2-isoprostanes in human urine are excreted as glucuronide conjugates. *Anal. Biochem.* **403,** 126–8 (2010).
16. Kamata, T., Nishikawa, M., Katagi, M. & Tsuchihashi, H. Optimized glucuronide hydrolysis for the detection of psilocin in human urine samples. *J. Chromatogr. B* **796,** 421–427 (2003).
17. Little, J. M. *et al.* Glucuronidation of oxidized fatty acids and prostaglandins B1 and E2 by human hepatic and recombinant UDP-glucuronosyltransferases. *J. Lipid Res.* **45,** 1694–1703 (2004).
18. Tsujikawa, K. *et al.* Optimized Conditions for the Enzymatic Hydrolysis of Glucuronide in Human Urine. **50,** 286–289 (2004).
19. Campbell, W. B., Holland, O. B., Adams, B. V & Gomez-Sanchez, C. E. Urinary excretion of prostaglandin E2, prostaglandin F2 alpha, and thromboxane B2 in normotensive and hypertensive subjects on varying sodium intakes. *Hypertension* **4,** 735–741 (2015).
20. Mucha, I. & Riutta, A. Determination of 9 α, 11 β -prostaglandin F2 in human urine. Combination of solid-phase extraction and radioimmunoassay. *Prostaglandins, Leukot. Essent. Fat. Acids* **65,** 271–280 (2001).
21. Frölich, J. C. *et al.* Urinary prostaglandins. Identification and origin. *J. Clin. Invest.* **55,** 763–70 (1975).
22. Newman, J. W., Watanabe, T. & Hammock, B. D. The simultaneous quantification of cytochrome P450 dependent linoleate and arachidonate metabolites in urine by HPLC-MS/MS. *J. Lipid Res.* **43,** 1563–1578 (2002).
23. Sterz, K., Scherer, G. & Ecker, J. A simple and robust UPLC-SRM/MS method to quantify urinary eicosanoids. *J. Lipid Res.* **53,** 1026–1036 (2012).
24. Barocas, D. A. *et al.* Oxidative stress measured by urine F2-isoprostane level is associated with prostate cancer. *J. Urol.* **185,** 2102–2107 (2011).
25. Medina, S. *et al.* A ultra-pressure liquid chromatography/triple quadrupole tandem mass spectrometry method for the analysis of 13 eicosanoids in human urine and quantitative 24 hour values in healthy volunteers in a controlled constant diet. *Rapid Commun. Mass Spectrom.* **26,** 1249–1257 (2012).
26. Welsh, T. N. *et al.* Optimization of a solid phase extraction procedure for prostaglandin E2, F2α and their tissue metabolites. *Prostaglandins Other Lipid Mediat.* **83,** 304–310 (2007).
27. Yan, W., Byrd, G. D. & Ogden, M. W. Quantitation of isoprostane isomers in human urine from smokers and nonsmokers by LC-MS/MS. *J. Lipid Res.* **48,** 1607–17 (2007).
28. Medina, S. *et al.* Assessment of oxidative stress markers and prostaglandins after chronic training of triathletes. *Prostaglandins Other Lipid Mediat.* **99,** 79–86 (2012).
29. Nair, S. C. *et al.* Does disease activity add to functional disability in estimation of utility for rheumatoid arthritis patients on biologic treatment? *Rheumatology (Oxford).* **55,** 94–102 (2016).
30. Taylor, J. I., Grace, P. B. & Bingham, S. a. Optimization of conditions for the enzymatic hydrolysis of phytoestrogen conjugates in urine and plasma. *Anal. Biochem.* **341,** 220–9 (2005).
31. Gomes, R. L., Meredith, W., Snape, C. E. & Sephton, M. A. Analysis of conjugated steroid androgens: deconjugation, derivatisation and associated issues. *J. Pharm. Biomed. Anal.* **49,** 1133–40 (2009).
32. Strassburg, K. *et al.* Quantitative profiling of oxylipins through comprehensive LC-MS/MS analysis: application in cardiac surgery. *Anal. Bioanal. Chem.* **404,** 1413–26 (2012).
33. Linting, M. & van der Kooij, A. Nonlinear Principal Components Analysis With CATPCA: A Tutorial. *J. Pers. Assess.* **94,** 12–25 (2012).
34. Shannon, P. *et al.* Cytoscape: a software environment for integrated models of biomolecular interaction networks. *Genome Res.* **13,** 2498–504 (2003).

35. Peters, F. T. & Remane, D. Aspects of matrix effects in applications of liquid chromatography-mass spectrometry to forensic and clinical toxicology--a review. *Anal. Bioanal. Chem.* **403,** 2155–72 (2012).
36. Salvatore, S. R. *et al.* Characterization and quantification of endogenous fatty acid nitroalkene metabolites in human urine. *J. Lipid Res.* **54,** 1998–2009 (2013).
37. Olson, M. V *et al.* Docosahexaenoic acid reduces inflammation and joint destruction in mice with collagen-induced arthritis. *Inflamm. Res.* **62,** 1003–1013 (2013).
38. Veselinovic, M. *et al.* Oxidative stress in rheumatoid arthritis patients: relationship to diseases activity. *Mol. Cell. Biochem.* **391,** 225–232 (2014).
39. Wruck, C. *et al.* Role of oxidative stress in rheumatoid arthritis: insights from the Nrf2-knockout mice. *Ann. Rheum. Dis.* **70,** 844–850 (2011).
40. Prevoo, M. *et al.* Modified disease activity scores that include twentyeight- joint counts: development and validation in a prospective longitudinal study of patients with rheumatoid arthritis. *Arthritis Rheum.* **38,** 44–48 (1995).
41. Isaacs, J. D. & Ferraccioli, G. The need for personalised medicine for rheumatoid arthritis. *Ann. Rheum. Dis.* **70,** 4–7 (2011).
42. Thomson, S. J., Askari, A. & Bishop-Bailey, D. Anti-inflammatory effects of epoxyeicosatrienoic acids. *Int. J. Vasc. Med.* **2012,** 1–7 (2012).

Chapter 3 Supplementary information

Supplementary Tables

Table S3.1. Overview of internal standards.

ISTD name	*m/z* Precursor ion -> Product ion
(±) 12,13-DiHOME-d4	317.3 -> 185.2
(±) 9,10-DiHOME-d4	317.3 -> 203.2
10-Nitrooleate-d17	343.1->46.05
12(S)-HETE-d8	327.3 -> 184.2
14,15-DiHETrE-d11	348.3 -> 207.1
15-deoxy-D-13,14-PGJ2-d4	319.2 -> 275.3
20-HETE-d6	325.3 -> 279.2
5(S)-HETE-d8	327.3 -> 116.1
5-iPF2a-VI-d11	364.2->115.05
6-keto PGF1a-d4	373.2 -> 167.2
8,12-iso-iPF2a-d11	364.2->115.05
8-iso-PGE2-d4	355.3->275.25
8-iso-PGF1a-d9	364.2->320.25
8-iso-PGF2a-d4	357.3->197.15
9(S)-HODE-d4	299.2 -> 172.1
iPF2a-VI-d4	357.2->114.9
KETE-d7	324.2 -> 280.3
LTB4-d4	339.2 -> 197.1
LTE4-d3	441.2 -> 336.2
PGA2-d4	336.9->275.0
PGD2-d4	355.2 -> 275.2
PGE1-d4	357.3->321.2
PGE2-d9	359.9->280.25
PGE2-d9	359.9->280.25
PGF2a-d4	357.3-> 197.2
TXB2-d4	373.2-> 173.1

Table S3.2. Complete COX pathway oxidised lipid target list

Metabolites	Precursor ion □ Product ion (*m/z*)	ISTD	Formal name	Lipidmaps ID	InChIKey
11beta-13,14-dihydro-15-keto-PGF2a	353.2 -> 113.2	(d4) PGF2a	9?,11?-dihydroxy-15-oxo-prost-5Z-en-1-oic acid	LMFA03010203	VKTIONYPMSCHQI-KGILNJEGSA-N
11beta-PGE2	351.2 -> 271.3	(d9) PGE2	9-oxo-11?,15S-dihydroxy-prosta-5Z,13E-dien-1-oic acid	LMFA03010060	XEYBRNLFEZDVAW-YUOXZBOXSA-N
11beta-PGF2a	353.2 -> 193.1	(d4) PGF2a	9α,11β,15S-trihydroxy-prosta-5Z,13E-dien-1-oic acid	LMFA03010036	PXGPLTODNUVGFL-ZWAKLXPCSA-N
12S-HHTrE	279.2 -> 179.2	(d8) 12(S)-HETE	12S-hydroxy-5Z,8E,10E-heptadecatrienoic acid	LMFA03050002	KUKJHGXXZWHSBG-WBGSEQOASA-N
13,14-dihydro-15-keto-PGD1	353.2 -> 209.1	(d4) PGD2	9α-hydroxy-11,15-dioxo-prost-1-oic acid	*na*	WTCAXDJXNVRHRC-KURKYZTESA-N
13,14-dihydro-15-keto-PGD2	351.2 -> 175.2	(d4) PGD2	9?-hydroxy-11,15-dioxo-prost-5Z-en-1-oic acid	LMFA03010022	VSRXYLYXIXYEST-KZTWKYQFSA-N
13,14-dihydro-15-keto-PGE2	351.2 -> 175.2	(d9) PGE2	9,15-dioxo-11?-hydroxy-prost-5Z-en-1-oic acid	LMFA03010031	CUJMXIQZWPZMNQ-XYYGWQPLSA-N
13,14-dihydro-15-keto-PGF1a	355.2 -> 193.2	(d4) PGF2a	9S,11R-dihydroxy-15-oxo-prostanoic acid	LMFA03010168	FVPKMMQYALWZHV-AKHDSKFASA-N
13,14-dihydro-15-keto-PGF2a	353.2 -> 183.1	(d4) PGF2a	9?,11?-dihydroxy-15-oxo-prost-5Z-en-1-oic acid	LMFA03010027	VKTIONYPMSCHQI-XAGFEHLVSA-N
13,14-dihydro-PGF2a	355.2 -> 275.3	(d4) PGF2a	9S,11R,15S-trihydroxy-5Z-prostenoic acid	LMFA03010079	LLQBSJQTCKVWTD-QPJJXVBHSA-N
15-deoxy-delta-12,14-PGD2	333.2 -> 271.2	(d4) PGD2	9?-hydroxy-11-oxo-prosta-5Z,12E,14E-trien-1-oic acid	LMFA03010051	QUGBPWLPAUHDTI-PLGLXCLHSA-N
15-keto-PGF1a	353.2 -> 221.1	(d4) PGF2a	9S,11R-dihydroxy-15-oxo-13E-prostaenoic acid	LMFA03010150	QPXXPLNAYDQELM-QNXXGYPUSA-N
15-keto-PGF2a	351.2 -> 219.1	(d4) PGF2a	9S,11R-dihydroxy-15-oxo-5Z,13E-prostadienoic acid	LMFA03010026	LOLJEILMPWPILA-AMFHKTBMSA-N
1a,1b-dihomo-PGF2a	381.3 -> 337.2	(d4) PGF2a	1a,1b-dihomo-9S,11R,15S-trihydroxy-5Z,13E-prostadienoic acid	LMFA03010157	ZCTAOAWRUXSOQF-GWSKAPOCSA-N
2,3-dinor-11b-PGF2a	325.2 -> 145.1	(d4) 8-iso-PGF2a	9α,11β,15S-trihydroxy-2,3-dinor-prosta-5Z,13E-dien-1-oic acid	LMFA03010011	IDKLJIUIJUVJNR-KSJYGFEGSA-N
20-hydroxy-PGE2	367.2 -> 287.2	(d9) PGE2	9-oxo-11?,15S,20-trihydroxy-prosta-5Z,13E-dien-1-oic acid	LMFA03010014	AZIGEYVZEVXWAD-NZGURKHLSA-N
20-hydroxy-PGF2a	369.2 -> 193.1	(d4) PGF2a	9S,11S,15S,20-tetrahydroxy-5Z,13E-prostadienoic acid	LMFA03010029	XQXUYZDBZCLAQO-UNKHNRNISA-N
6-keto PGE1	367.2 -> 143.1	(d4) 6-keto PGF1a	6,9-dioxo-11R,15S-dihydroxy-13E-prostenoic acid	LMFA03010012	ROUDCKODIMKLNO-CTBSXBMHSA-N
6-keto-PGF1a	369.2 -> 163.1	(d4) 6-keto PGF1a	6-oxo-9?,11?,15S-trihydroxy-prost-13E-en-1-oic acid	LMFA03010001	KFGOFTHODYBSGM-ZUNNJUQCSA-N
bicyclo-PGE2	333.2 -> 113.2	(d9) PGE2	11-deoxy-13,14-dihydro-15-keto-11?,16.xi.-cycloprostaglandin E2	LMFA03010034	CGCZPIJMGKLVTQ-PAJBVNRRSA-N
d12-PGJ2	333.2 -> 233.1	(d4) 15-deoxy-D-13,14-PGJ2	11-oxo-15S-hydroxy-prosta-5Z,9,12E-trien-1-oic acid	LMFA03010020	TUXFWOHFPFBNEJ-GJGHEGAFSA-N
D17, 6-ketoPGF1a	367.2 -> 163.1	(d4) 6-keto PGF1a	6-oxo-9S,11R,15S-trihydroxy-13E,17Z-prostadienoic acid	LMFA03010149	HFKNJQYMAGMXTR-CAPHXMBKSA-N
PGA1	335.1 -> 273.15	(d4) PGA2	9-oxo-15S-hydroxy-10Z,13E-prostadienoic acid	LMFA03010005	BGKHCLZFGPIKKU-LDDQNKHRSA-N

PGA2	333.2 -> 271.2	(d4) PGA2	9-oxo-15S-hydroxy-5Z,10Z,13E-prostatrienoic acid	LMFA03010035	MYHXHCUNDDAEOZ-FOSBLDSVSA-N
PGD1	353.2 -> 273.2	(d4) PGD2	9?,15S-dihydroxy-11-oxo-prost-13E-en-1-oic acid	LMFA03010049	CIMMACURCPXICP-PNQRDDRVSA-N
PGD2	351.2 -> 271.2	(d4) PGD2	9S,15S-dihydroxy-11-oxo-5Z,13E-prostadienoic acid	LMFA03010004	BHMBVRSPMRCCGG-OUTUXVNYSA-N
PGD3	349.2 -> 269.2	(d4) PGD2	9S,15S-dihydroxy-11-oxo-5Z,13E,17Z-prostatrienoic acid	LMFA03010142	ANOICLBSJIMQTA-WXGBOJPQSA-N
PGE1	353.2 -> 273.2	(d4) PGE1	9-oxo-11R,15S-dihydroxy-13E-prostaenoic acid	LMFA03010134	GMVPRGQOIOIIMI-DWKJAMRDSA-N
PGE2	351.2 -> 271.2	(d9) PGE2	9-oxo-11R,15S-dihydroxy-5Z,13E-prostadienoic acid; Prostin E2	LMFA03010003	XEYBRNLFEZDVAW-ARSRFYASSA-N
PGE3	349.2 -> 269.2	(d9) PGE2	9-oxo-11R,15S-dihydroxy-5Z,13E,17Z-prostatrienoic acid	LMFA03010135	CBOMORHDRONZRN-QLOYDKTKSA-N
PGF1a	355.2 -> 293.2	(d4) PGF2a	9S,11R,15S-trihydroxy-13E-prostaenoic acid	LMFA03010137	DZUXGQBLFALXCR-CDIPTNKSSA-N
PGF2a	353.2 -> 193.1	(d4) PGF2a	9S,11R,15S-trihydroxy-5Z,13E-prostadienoic acid	LMFA03010002	PXGPLTODNUVGFL-YNNPMVKQSA-N
PGF3a	351.2 -> 193.2	(d4) PGF2a	9α,11α,15S-trihydroxy-prosta-5Z,13E,17Z-trien-1-oic acid	LMFA03010138	SAKGBZWJAIABSY-SAMSIYEGSA-N
PGJ2	333.2 -> 233.1	(d4) PGD2	11-oxo-15S-hydroxy-prosta-5Z,9,13E-trien-1-oic acid	LMFA03010019	UQOQENZZLBSFKO-POPPZSFYSA-N
PGK2	349.2 -> 205.1	(d9) PGE2	9,11-dioxo-15S-hydroxy-5Z,13E-prostadienoic acid	LMFA03010023	LGMXPVXJSFPPTQ-DJUJBXLVSA-N
Tetranor-PGEM	327.1 -> 309.2	(d9) PGE2	11R-hydroxy-9,15-dioxo-2,3,4,5-tetranor-prostan-1,20-dioic acid	LMFA03010032	ZJAZCYLYLVCSNH-JHJVBQTASA-N
Tetranor-PGFM	329.2 -> 311.2	(d4) PGF2a	9S,11R-dihydroxy-15-oxo-2,3,4,5-tetranor-prostan-1,20-dioic acid	LMFA03010139	IGRHJCFWWOQYQE-SYQHCUMBSA-N
TXB1	371.2 -> 171.1	(d4) TXB2	9S,11,15S-trihydroxy-thrombox-13E-enoic acid	LMFA03030008	JSDWWNLTJCCSAV-RLBQWBRQSA-N
TXB2	369.2 -> 169.1	(d4) TXB2	9S,11,15S-trihydroxy-thromboxa-5Z,13E-dien-1-oic acid	LMFA03030002	XNRNNGPBEPRNAR-JQBLCGNGSA-N
TXB3	367.2 -> 169.1	(d4) TXB2	9S,11,15S-trihydroxy-thromboxa-5Z,13E,17Z-trien-1-oic acid	LMFA03030006	OYPPJMLKAYYWHH-NXJDUNGTSA-N

Table S3.3: Complete CYP pathway oxidised lipid target list

Metabolites	Precursor ion □ Product ion (*m/z*)	ISTD	Formal name	Lipidmaps ID	InChIKey
11,12-DiHETrE	337.2 -> 167.2	(d11) 14,15-DiHETrE	(±)11,12-dihydroxy-5Z,8Z,14Z-eicosatrienoic acid	LMFA03050008	LRPPQRCHCPFBPE-LZXKBWHHSA-N
11,12-EpETrE	319.2 -> 167.1	(d11) 14,15-DiHETrE	(±)11(12)-epoxy-5Z,8Z,14Z-eicosatrienoic acid	LMFA03080014	DXOYQVHGIODESM-LZXKBWHHSA-N
12,13-DiHODE	311.2 -> 293.0	(d4) 9(S)-HODE	(+/-)-12,13-dihydroxy-9Z,15Z-octadecadienoic acid	LMFA02000046	RGRKFKRAFZJQMS-OOHFSOINSA-N
12,13-DiHOME	313.2 -> 183.2	(d4) 12,13-DiHOME	12,13-dihydroxy-9Z-octadecenoic acid	LMFA01050351	CQSLTKIXAJTQGA-GJGKEFFFSA-N
12,13-EpOME	295.2 -> 195.2	(d4) 12,13-DiHOME	(+/-)-12(13)-epoxy-9Z-octadecenoic acid	LMFA02000038	CCPPLLJZDQAOHD-FLIBITNWSA-N
14,15-DiHETE	335.2 -> 207.1	(d11) 14,15-DiHETrE	14,15-dihydroxy-5Z,8Z,11Z,17Z-eicosatetraenoic acid	LMFA03060077	BLWCDFIELVFRJY-IXQKDQKQSA-N
14,15-DiHETrE	337.2 -> 207.2	(d11) 14,15-DiHETrE	(±)14,15-dihydroxy-5Z,8Z,11Z-eicosatrienoic acid	LMFA03050010	SYAWGTIVOGUZMM-KZTFMOQPSA-N
14,15-EpETE	317.2 -> 207.1	(d11) 14,15-DiHETrE	(±)14(15)-epoxy-5Z,8Z,11Z,17Z-eicosatetraenoic acid	LMFA03000003	RGZIXZYRGZWDMI-IXQKDQKQSA-N
14,15-EpETrE	319.2 -> 219.2	(d11) 14,15-DiHETrE	(±)14(15)-epoxy-5Z,8Z,11Z-eicosatrienoic acid	LMFA03080013	JBSCUHKPLGKXKH-KZTFMOQPSA-N
16,17-EpDPE	343.2 -> 233.2	(d11) 14,15-DiHETrE	(±)16(17)-epoxy-4Z,7Z,10Z,13Z,19Z-docosapentaenoic acid	LMFA04000037	BCTXZWCPBLWCRV-QCAYAECISA-N
17,18-DiHETE	335.2 -> 247.2	(d11) 14,15-DiHETrE	(+/-)-17,18-dihydroxy-5Z,8Z,11Z,14Z-eicosatetraenoic acid	LMFA03060078	XYDVGNAQQFWZEF-JPURVOHMSA-N
17,18-EpETE	317.2 -> 259.2	(d11) 14,15-DiHETrE	(+/-)-17(18)-epoxy-5Z,8Z,11Z,14Z-eicosatetraenoic acid	LMFA03000004	GPQVVJQEBXAKBJ-JPURVOHMSA-N
19,20-DiHDPA	361.2 -> 273.3	(d11) 14,15-DiHETrE	(±)19,20-dihydroxy-4Z,7Z,10Z,13Z,16Z-docosapentaenoic acid	LMFA04000043	FFXKPSNQCPNORO-MBYQGORISA-N
20-HETE	319.2 -> 289.2	(d6) 20-HETE	20-hydroxy-5Z,8Z,11Z,14Z-eicosatetraenoic acid	LMFA03060009	NNDIXBJHNLFJJP-DTLRTWKJSA-N
5,6-DiHETrE	337.2 -> 145.1	(d11) 14,15-DiHETrE	5S,6S-dihydroxy-7E,9E,11Z,14Z-eicosatetraenoic acid	LMFA03060018	UVZBUUTTYHTDRR-WAQVJNLQSA-N
5,6-EpETrE	319.2 -> 191.2	(d11) 14,15-DiHETrE	(±)5(6)-epoxy-8Z,11Z,14Z-eicosatrienoic acid	LMFA03080017	VBQNSZQZRAGRIX-GSKBNKFLSA-N
5S,6S-DiHETE	335.2 -> 115.1	(d4) LTB4	5S,6S-dihydroxy-7E,9E,11Z,14Z-eicosatetraenoic acid	LMFA03060018	UVZBUUTTYHTDRR-WAQVJNLQSA-N
8,9-DiHETrE	337.2 -> 127.0	(d11) 14,15-DiHETrE	8,9-dihydroxy-5Z,11Z,14Z-eicosatrienoic acid	LMFA03050006	DCJBINATHQHPKO-TYAUOURKSA-N
8,9-EpETrE	319.2 -> 155.1	(d11) 14,15-DiHETrE	(±)8(9)-epoxy-5Z,11Z,14Z-eicosatrienoic acid	LMFA03080019	DBWQSCSXHFNTMO-ZZMPYBMWSA-N
9,10-DiHOME	313.2 -> 201.1	(d4) 9,10-DiHOME	9,10-dihydroxy-12Z-octadecenoic acid	LMFA02000229	XEBKSQSGNGRGDW-CJWPDFJNSA-N
9,10-EpOME	295.2 -> 171.2	(d4) 9,10-DiHOME	(+/-)-9(10)-epoxy-12Z-octadecenoic acid	LMFA02000037	FBUKMFOXMZRGRB-XKJZPFPASA-N

Table S3.4: Complete LOX pathway oxidised lipid target list

Metabolites	Precursor ion □ Product ion (*m/z*)	ISTD	Formal name	Lipidmaps ID	InChIKey
10S,17S-DiHDoHE	359.2 -> 153.2	(d4) LTB4	10(S),17(S)-dihydroxy-4Z,7Z,11E,13Z,15E,19Z-docosahexaenoic acid	LMFA04000047	CRDZYJSQHCXHEG-XLBFCUQGSA-N
11-trans-LTC4	624.3 -> 272.1	(d4) LTE4	5S-hydroxy-6R-(S-glutathionyl)-7E,9E,11E,14Z-eicosatetraenoic acid	LMFA03020020	GWNVDXQDILPJIG-GXMXCQGXSA-N
11-trans-LTD4	495.2 -> 177.1	(d4) LTE4	5S-hydroxy-6R-(S-cysteinylglycinyl)-7E,9E,11E,14Z-eicosatetraenoic acid	LMFA03020021	YEESKJGWJFYOOK-XILINCIBSA-N
11-trans-LTE4	438.2 -> 333.2	(d4) LTE4	5S-hydroxy-6R-(S-cysteinyl)-7E,9E,11E14Z-eicosatetraenoic acid	LMFA03020022	OTZRAYGBFWZKMX-DVFCZEDWSA-N
12-HETE	319.2 -> 179.2	(d8) 12(S)-HETE	12-hydroxy-5Z,8Z,10E,14Z-eicosatetraenoic acid	LMFA03060088	ZNHVWPKMFKADKW-VXBMJZGYSA-N
12-KETE	317.2 -> 273.3	(d7) KETE	12-oxo-5Z,8Z,10E,14Z-eicosatetraenoic acid	LMFA03060019	GURBRQGDZZKITB-VXBMJZGYSA-N
12S-HEPE	317.2 -> 179.1	(d8) 12(S)-HETE	12S-hydroxy-5Z,8Z,10E,14Z,17Z-eicosapentaenoic acid	LMFA03070008	MCRJLMXYVFDXLS-UOLHMMFFSA-N
12S-HpETE	317.2 -> 273.3	(d8) 12(S)-HETE	12S-hydroperoxy-5Z,8Z,10E,14Z-eicosatetraenoic acid	LMFA03060013	ZIOZYRSDNLNNNJ-VXBMJZGYSA-N
13-HODE	295.2 -> 195.2	(d4) 9(S)-HODE	13S-hydroxy-9Z,11E-octadecadienoic acid	LMFA02000154	HNICUWMFWZBIFP-BSZOFBHHSA-N
13-HpODE	311.2 -> 113.2	(d4) 9(S)-HODE	(±)13-hydroperoxy-9Z,11E-octadecadienoic acid	LMFA02000034	JDSRHVWSAMTSSN-BSZOFBHHSA-N
13-KODE	293.2 -> 113.1	(d4) 9(S)-HODE	13-keto-9Z,11E-octadecadienoic acid	LMFA02000016	JHXAZBBVQSRKJR-BSZOFBHHSA-N
14,15-LTC4	624.3 -> 272.1	(d4) LTE4	15S-hydroxy-14R-(S-glutathionyl)-5Z,8Z,10E,12E-eicosatetraenoic acid	LMFA03020031	OBQVBASHEWLKCQ-JTLMKIFUSA-N
14,15-LTE4	438.2 -> 333.2	(d4) LTE4	15S-hydroxy,14R-(S-cysteinyl)-5Z,8Z,10E,12E-eicosatetraenoic acid	LMFA03020033	JLJNENVYAVKECZ-HRXVJLLUSA-N
15-HETE	319.2 -> 219.2	(d8) 5(S)-HETE	15S-hydroxy-5Z,8Z,11Z,13E-eicosatetraenoic acid	LMFA03060001	JSFATNQSLKRBCI-VAEKSGALSA-N
15-HpETE	335.2 -> 113.1	(d8) 5(S)-HETE	15S-hydroperoxy-5Z,8Z,11Z,13E-eicosatetraenoic acid	LMFA03060014	BFWYTORDSFIVKP-VAEKSGALSA-N
15-KETE	317.2 -> 113.2	(d7) KETE	15-oxo-5Z,8Z,11Z,13E-eicosatetraenoic acid	LMFA03060051	YGJTUEISKATQSM-USWFWKISSA-N
15S-HEPE	317.2 -> 219.2	(d8) 5(S)-HETE	15S-hydroxy-5Z,8Z,11Z,13E,17Z-eicosapentaenoic acid	LMFA03070009	WLKCSMCLEKGITB-DBVSHIMFSA-N
15S-HETrE	321.2 -> 221.2	(d8) 5(S)-HETE	15S-hydroxy-8Z,11Z,13E-eicosatrienoic acid	LMFA03050007	IUKXMNDGTWTNTP-OAHXIXLCSA-N
20-carboxy-LTB4	365.2 -> 347.2	(d4) LTB4	5S,12R-dihydroxy-6Z,8E,10E,14Z-eicosatetraene-1,20-dioic acid	LMFA03020016	SXWGPVJGNOLNHT-VFLUTPEKSA-N
20-hydroxy-LTB4	351.2 -> 195.1	(d4) LTB4	5S,12R,20-trihydroxy-6Z,8E,10E,14Z-eicosatetraenoic acid	LMFA03020018	PTJFJXLGRSTECQ-PSPARDEHSA-N
5-HETE	319.2 -> 115.1	(d8) 5(S)-HETE	5S-hydroxy-6E,8Z,11Z,14Z-eicosatetraenoic acid	LMFA03060002	KGIJOOYOSFUGPC-JGKLHWIESA-N
5-HETrE	321.3 -> 303.0	(d8) 5(S)-HETE	5S-hydroxy-6E,8Z,11Z-eicosatrienoic acid	LMFA03050005	LSADDRSUZRRBAN-FDSUASFTSA-N
5-KETE	317.2 -> 203.2	(d7) KETE	5-oxo-6E,8Z,11Z,14Z-eicosatetraenoic acid	LMFA03060011	MEASLHGILYBXFO-XTDASVJISA-N

5S,14R-Lipoxin B4	351.2 -> 221.2	(d4) LTB4	5S,14R,15S-trihydroxy-6E,8Z,10E,12E-eicosatetraenoic acid	LMFA03040002	UXVRTOKOJOMENI-WLPVFMORSA-N
5S,15S-DiHETE	335.2 -> 115.1	(d4) LTB4	5S,15S-dihydroxy-6E,8Z,10Z,13E-eicosatetraenoic acid	LMFA03060010	UXGXCGPWGSUMNI-BVHTXILBSA-N
5S,6R-LipoxinA4	351.2 -> 115.1	(d4) LTB4	5S,6R,15S-trihydroxy-7E,9E,11Z,13E-eicosatetraenoic acid	LMFA03040001	IXAQOQZEOGMIQS-SSQFXEBMSA-N
5S,6S-Lipoxin A4	351.2 -> 115.1	(d4) LTB4	5S,6R,15S-trihydroxy-7E,9E,11Z,13E-eicosatetraenoic acid	LMFA03040001	IXAQOQZEOGMIQS-SSQFXEBMSA-N
5S-HEPE	317.2 -> 115.1	(d8) 5(S)-HETE	5S-hydroxy-6E,8Z,11Z,14Z,17Z-eicosapentaenoic acid	LMFA03070010	FTAGQROYQYQRHF-GHWNLOBHSA-N
5S-HpETE	317.3 -> 203.2	(d8) 5(S)-HETE	5S-hydroperoxy-6E,8Z,11Z,14Z-eicosatetraenoic acid	LMFA03060012	JNUUNUQHXIOFDA-JGKLHWIESA-N
6-trans-LTB4	335.2 -> 195.2	(d4) LTB4	5S,12R-dihydroxy-6E,8E,10E,14Z-eicosatetraenoic acid	LMFA03020013	VNYSSYRCGWBHLG-UKNWISKWSA-N
8-HETrE	321.3 -> 303.0	(d8) 12(S)-HETE	8S-hydroxy-9E,11Z,14Z-eicosatrienoic acid	LMFA03050011	SKIQVURLERJJCK-RDCCVJQZSA-N
8S,15S-DiHETE	335.2 -> 235.2	(d4) LTB4	8S,15S-dihydroxy-5Z,9E,11Z,13E-eicosatetraenoic acid	LMFA03060050	NNPWRKSGORGTIM-HCCKYKKOSA-N
9,10,13-TriHOME	329.2 -> 171.1	(d4) 9(S)-HODE	E)-9,10,13-Trihydroxy-11-octadecenoic acid	LMFA02000168	NTVFQBIHLSPEGQ-BUHFOSPRSA-N
9,12,13-TriHOME	329.2 -> 211.2	(d4) 9(S)-HODE	9S,12S,13S-trihydroxy-10E-octadecenoic acid	LMFA02000014	MDIUMSLCYIJBQC-MVFSOIOZSA-N
9-HODE	295.2 -> 171.1	(d4) 9(S)-HODE	(±)-9-hydroxy-10E,12Z-octadecadienoic acid	LMFA02000151	NPDSHTNEKLQQIJ-ZJHFMPGASA-N
9-HOTrE	293.2 -> 171.1	(d4) 9(S)-HODE	9S-hydroxy-10E,12Z,15Z-octadecatrienoic acid	LMFA02000024	RIGGEAZDTKMXSI-MEBVTJQTSA-N
9-HpODE	311.2 -> 185.2	(d4) 9(S)-HODE	9S-hydroperoxy-10E,12Z-octadecadienoic acid	LMFA02000012	JGUNZIWGNMQSBM-UINYOVNOSA-N
9-KODE	293.2 -> 185.2	(d4) 9(S)-HODE	9-oxo-10E,12Z-octadecadienoic acid	LMFA02000274	LUZSWWYKKLTDHU-ZJHFMPGASA-N
Hepoxilin A3	335.2 -> 273.2	(d8) 12(S)-HETE	8-hydroxy-11S,12S-epoxy-5Z,14Z,9E-eicosatrienoic acid	LMFA03090005	SGTUOBURCVMACZ-SEVPPISGSA-N
LTB4	335.2 -> 195.1	(d4) LTB4	5S,12R-dihydroxy-6Z,8E,10E,14Z-eicosatetraenoic acid	LMFA03020001	VNYSSYRCGWBHLG-AMOLWHMGSA-N
LTB5	333.2 -> 195.1	(d4) LTB4	5S,12S-dihydroxy-6Z,8E,14Z,17Z-eicosapentanenoic acid	LMFA03020010	BISQPGCQOHLHQK-HDNPQISLSA-N
LTC4	624.3 -> 272.1	(d4) LTE4	5S-hydroxy-6R-(S-glutathionyl)-7E,9E,11Z,14Z-eicosatetraenoic acid	LMFA03020003	GWNVDXQDILPJIG-SWOVEEFNSA-N
LTD4	495.2 -> 177.1	(d4) LTE4	5S-hydroxy-6R-(S-cysteinylglycinyl)-7E,9E,11Z,14Z-eicosatetraenoic acid	LMFA03020077	YEESKJGWJFYOOK-LDDGIIIKSA-N
LTE4	438.2 -> 333.2	(d4) LTE4	5S-hydroxy,6R-(S-cysteinyl),7E,9E,11Z,14Z-eicosatetraenoic acid	LMFA03020002	OTZRAYGBFWZKMX-FRFVZSDQSA-N
Resolvin D1	375.2 -> 141.0	(d4) LTB4	7S,8R,17S-trihydroxy-4Z,9E,11E,13Z,15E,19Z-docosahexaenoic acid	LMFA04000006	OIWTWACQMDFHJG-CCFUIAGSSA-N

Table S3.5: Complete ROS/RNS pathway oxidised lipid target list

Metabolites	Precursor ion □ Product ion (*m/z*)	ISTD	Formal name	Lipidmaps ID	InChIKey
NO2-aLA (C18:3)	322.1 -> 46.05	10-Nitrooleate-d17	nitro-9E,12Z,15Z-octadecadienoic acid	*na*	*na*
NO2-LA (C18:2)	324.3 -> 277.25	10-Nitrooleate-d17	nitro-9E,12Z-octadecadienoic acid	LMFA01120001	LELVHAQTWXTCLY-XYWKCAQWSA-N
NO2-OA (C18:1)	326.1 -> 46.0	10-Nitrooleate-d17	nitro-9E-octadecenoic acid	LMFA01120003	WRADPCFZZWXOTI-BMRADRMJSA-N
10-HDoHE	343.2 -> 153.0	(d8) 12(S)-HETE	(+/-)-10-hydroxy-4Z,7Z,11E,13Z,16Z,19Z-docosahexaenoic acid	LMFA04000027	DDCYKEYDTGCKAS-SKSHMZPZSA-N
11-HDoHE	343.2 -> 121.0	(d8) 12(S)-HETE	(+/-)-11-hydroxy-4Z,7Z,9E,13Z,16Z,19Z-docosahexaenoic acid	LMFA04000028	LTERDCBCHFKFRI-BGKMTWLOSA-N
11-HETE	319.2 -> 167.1	(d8) 12(S)-HETE	11R-hydroxy-5Z,8Z,12E,14Z-eicosatetraenoic acid	LMFA03060028	GCZRCCHPLVMMJE-WXMXURGXSA-N
13-HDoHE	343.2 -> 281.0	(d8) 12(S)-HETE	(+/-)-13-hydroxy-4Z,7Z,10Z,14E,16Z,19Z-docosahexaenoic acid	LMFA04000029	SEVOKGDVLLIUMT-SKSHMZPZSA-N
14-HDoHE	343.2 -> 205.0	(d8) 12(S)-HETE	(+/-)-14-hydroxy-4Z,7Z,10Z,12E,16Z,19Z-docosahexaenoic acid	LMFA04000030	ZNEBXONKCYFJAF-BGKMTWLOSA-N
16-HDoHE	343.2 -> 233.0	(d8) 12(S)-HETE	(±)16-hydroxy-4Z,7Z,10Z,13Z,17E,19Z-docosahexaenoic acid	LMFA04000031	CSXQXWHAGLIFIH-VUARBJEWSA-N
17-HDoHE	343.2 -> 281.3	(d8) 12(S)-HETE	(±)17-hydroxy-4Z,7Z,10Z,13Z,15E,19Z-docosahexaenoic acid	LMFA04000032	SWTYBBUBEPPYCX-VIIQGJSXSA-N
18-HEPE	317.2 -> 255.0	(d8) 12(S)-HETE	(±)-18-hydroxy-5Z,8Z,11Z,14Z,16E-eicosapentaenoic acid	LMFA03070033	LRWYBGFSVUBWMO-UXNZXXPISA-N
2,3-dinor-8-iso-PGF2a	325.1 -> 237.2	(d4) 8-iso-PGF2a	9α,11α,15S-trihydroxy-2,3-dinor-(8β)-prosta-5Z,13E-dien-1-oic acid	LMFA03110010	IDKLJIUIJUVJNR-JSEKUSAISA-N
20-HDoHE	343.2 -> 299.0	(d8) 12(S)-HETE	(+/-)-20-hydroxy-4Z,7Z,10Z,13Z,16Z,18E-docosahexaenoic acid	LMFA04000033	YUZXOJOCNGKDNI-LFVREGEGSA-N
4-HDoHE	343.2 -> 281.0	(d8) 12(S)-HETE	(±)4-hydroxy-5E,7Z,10Z,13Z,16Z,19Z-docosahexaenoic acid	LMFA04000024	IFRKCNPQVIJFAQ-PQVBWYSWSA-N
(+/-) 5-iPF2a VI	353.3 -> 115.05	(d11) 5-iPF2a IV	5,9S,11R-trihydroxy-6E,14Z-prostadienoic acid-cyclo[8S,12R]	LMFA03110011	RZCPXIZGLPAGEV-SUHLLOIRSA-N
7-HDoHE	343.2 -> 281.0	(d8) 12(S)-HETE	(±)7-hydroxy-4Z,8E,10Z,13Z,16Z,19Z-docosahexaenoic acid	LMFA04000025	OZXAIGIRPOOJTI-XJAVJPOHSA-N
8,12-iPF2a VI	353.3 -> 115.05	(d11) 8,12-iPF2a IV	(±)5,9α-trihydroxy-12α-prosta-6E,14Z-dien-1-oic acid	*na*	RZCPXIZGLPAGEV-DCOIXEBESA-N
8_HDoHE	343.2 -> 189.0	(d8) 12(S)-HETE	(±)8-hydroxy-4Z,6E,10Z,13Z,16Z,19Z-docosahexaenoic acid	LMFA04000026	ZHBVYDMSPDDAKE-VTIZNUJUSA-N
8-HETE	319.2 -> 155.1	(d8) 5(S)-HETE	(±)8-hydroxy-5Z,9E,11Z,14Z-eicosatetraenoic acid	LMFA03060086	NLUNAYAEIJYXRB-HEJOTXCHSA-N
8-iso-13,14-dihydro-PGF2a	353.3 -> 183.1	(d4) 8-iso-PGF2a	9S,11R-dihydroxy-15-oxo-5Z-prostaenoic acid-cyclo[8S,12R]	LMFA03110004	VKTIONYPMSCHQI-JPRPWBOBSA-N
8-iso-15-keto-PGE2	349.1 -> 287.2	(d4) 8-iso-PGE2	9,15-dioxo-11α-hydroxy-(8β)-prosta-5Z,13E-1-oic acid	LMFA03110009	YRTJDWROBKPZNV-RSNVZYGJSA-N
8-iso-15-keto-PGF2a	351.1 -> 315.15	(d4) 8-iso-PGF2a	9α,11α-dihydroxy-15-oxo-(8β)-prosta-5Z,13E-dien-1-oic acid	LMFA03110005	LOLJEILMPWPILA-RLXHZABYSA-N
8-iso-15-keto-PGF2b	351.1 -> 315.15	(d4) 8-iso-PGF2a	9β,11α-dihydroxy-15-oxo-(8β)-prosta-5Z,13E-dien-1-oic acid	*na*	*na*
8-iso-15(R)-PGF2a	353.3 -> 193.2	(d4) 8-iso-PGF2a	9α,11α,15R-trihydroxy-(8β)-prosta-5Z,13E-dien-1-oic acid	LMFA03110030	PXGPLTODNUVGFL-

					PGWUFSIFSA-N
8-iso-PGA1	335.1 -> 273.15	(d4) PGA2	9-oxo-15S-hydroxy-(8β)-prosta-10,13E-dien-1-oic acid	LMFA03110008	BGKHCLZFGPIKKU-DRSVPBQLSA-N
8-iso-PGA2	333.1 -> 271.2	(d4) PGA2	9-oxo-15S-hydroxy-(8β)-prosta-5Z,10,13E-trien-1-oic acid	LMFA03110140	MYHXHCUNDDAEOZ-UKUWKSPLSA-N
8-iso-PGE1	353.3 -> 317.2	(d4) PGE1	9-oxo-11α,15S-dihydroxy-(8β)-prost-13E-en-1-oic acid	LMFA03110002	GMVPRGQOIOIIMI-JCPCGATGSA-N
8-iso-PGE2	351.1 -> 271.15	(d4) 8-iso-PGE2	9-oxo-11α,15S-dihydroxy-(8β)-prosta-5Z,13E-dien-1-oic acid	LMFA03110003	XEYBRNLFEZDVAW-CLQOMRTCSA-N
8-iso-PGF1a	355.3 -> 311.1	(d9) 8-iso-PGF1a	9α,11α,15S-trihydroxy-(8β)-prost-13E-en-1-oic acid	*na*	DZUXGQBLFALXCR-PUCCXBQTSA-N
8-iso-PGF2a (15-F2t-IsoP)	353.3 -> 193.2	(d4) 8-iso-PGF2a	9α,11α,15S-trihydroxy-(8β)-prosta-5Z,13E-dien-1-oic acid	LMFA03110001	PXGPLTODNUVGFL-NAPLMKITSA-N
8-iso-PGF3a	351.1 -> 307.15	(d4) 8-iso-PGF2a	9α,11α,15S-trihydroxy-(8β)-prosta-5Z,13E,17Z-dien-1-oic acid	*na*	*na*
9-HEPE	317.2 -> 149.0	(d8) 12(S)-HETE	(±)-9-hydroxy-5Z,7E,11Z,14Z,17Z-eicosapentaenoic acid	LMFA03070029	OXOPDAZWPWFJEW-IMCWFPBLSA-N
9-HETE	319.2 -> 167.1	(d8) 12(S)-HETE	(±)-9-hydroxy-5Z,7E,11Z,14Z-eicosatetraenoic acid	LMFA03060089	KATOYYZUTNAWSA-OIZRIKEUSA-N
iPF2a-iV	353.3 -> 127.1	(d4) iPFa-VI	*na*	*na*	MZYZWZXTHYCVHQ-QXCZDIPSSA-N

Table S3.7 The GUS blank effect compared to non-hydrolysed urine.

GUS	8-iso-15(R)-PGF_{2a}	8-iso-13,14-dihydro-PGF_{2a}	8-iso-PGF_{2a}	PGE_2	PGE_1	PGF_{2a}	13,14-dihydro-PGF_{2a}	NO_2-linoleic acid	NO_2-oleic acid
H. pomatia	42.15	0.00	41.76	2.64	0.06	128.39	0.00	0.00	0.00
Bovine liver	0.00	0.00	21.18	0.05	0.05	16.12	0.00	0.00	0.00
E. coli	0.00	0.00	0.00	0.06	0.00	16.80	0.00	0.00	0.00

The GUS blank effect is calculated by: Metabolite response $_{\text{Enzyme blank}}$/ Metabolite response $_{\text{Urine}}$ ×100%

Table S3.6 The selected panel of compounds

Pathway	Metabolites	*m/z* Precursor ion -> Product ion	ISTD
COX	13,14-dihydro-PGF2a	353.30 -> 183.10	(d4) PGF2a
	PGE1	353.30 -> 317.20	(d4) PGE1
	PGE2	351.10 -> 271.15	(d9) PGE2
	PGF2a	353.30 -> 193.20	(d4) PGF2a
ROS	8-iso-13,14-dihydro-PGF2a	353.30 -> 183.10	(d4) 8-iso-PGF2a
	8-iso-15(R)-PGF2a	353.30 -> 193.20	(d4) 8-iso-PGF2a
	8-iso-PGF2a	353.30 -> 193.20	(d4) 8-iso-PGF2a
RNS	NO2-LA (C18:2)	324.30 -> 277.25	10-Nitrooleate-d17
	NO2-OA (C18:1)	326.10 -> 46.00	10-Nitrooleate-d17

Table S3.8 RSDs of free and total oxidized lipids measured in RA patient urine

Compound name	RSD (%)	
	Total oxidized lipid	Free oxidized lipid
8,12-iPF2a IV	2.31	1.72
12,13-DiHOME	6.98	2.78
9,10-DiHOME	1.91	2.9
iPF2a Unknown	5.86	4.49
PGF2a	7.21	4.88
2_3-dinor-8-iso-PGF2a	12.36	5.49
5-iPF2a IV	2.8	5.71
9,10-EpOME	20.51	7.03
PGA2		7.31
9-HODE	5.04	7.37
9,12,13-TriHOME	9.95	7.71
D17, 6-ketoPGF1a	7.97	8.41
8,9-DiHETrE	4.43	8.64
13-KODE	9.12	9.12
12-HETE	9.35	9.4
13-HODE	7	9.96
8-iso-PGF1a	11.97	10.05
PGF1a	23.33	10.17
20-carboxy-LTB4	13.96	10.18
14,15-DiHETrE	4.24	11.04
8-iso-PGF2a	17.37	11.1
9-HOTrE	4.2	11.82
5-iPF2a-VI	11.46	11.85
PGE1		11.9
9,10,13-TriHOME	7.09	13.22
8-iso-15(R)-PGF2a	5.66	13.38
12,13-EpOME	32.38	13.8
2,3-dinor-11b-PGF2a	14.54	16.72
13_14-dihydro-PGF2a	13.49	18.19
bicyclo-PGE2	13.84	19.93
14-HDoHE	25.99	19.97
PGE2	11.63	20.86
11beta-13,14-dihydro-15-keto-PGF2a	16.83	20.97
11beta-PGF2a	21.92	23.49
NO2-LA		23.56
8-iso-PGF2a	23.8	23.85
5S,6R-LipoxinA4	14.72	25.29
9-KODE	25.86	25.6
5S-HEPE	6.66	26.29
NO2-aLA		26.33
12S-HEPE	19.08	26.57
PGF2a	9.49	26.83
NO2-OA		50.11
8-iso-PGE1		22.85
19,20-DiHDPA	5.1	

9-HEPE	6.96
15S-HETrE	7.82
11,12-DiHETrE	8.05
PGK2	8.1
5,6-DiHETrE	9.7
17,18-DiHETE	10.24
12,13-DiHODE	11.97
PGF3a	12.63
20-HETE	12.64
PGE3	13.39
20-HDoHE	14.14
5-HETE	14.71
2_3-dinor-11b-PGF2a	14.74
9-HETE	14.86
iPF2a	15.55
8-HETE	16.58
11,12-EpETrE	17
10-HDoHE	17.14
15-HETE	17.64
13,14-dihydro-15-keto-PGE2	20.19
11-HDoHE	20.44
11-HETE	21.19
PGD3	21.98
14,15-DiHETE	22.37
8_HDoHE	23.31
5S,15S-DiHETE	23.9
16-HDoHE	24.46
13,14-dihydro-15-keto-PGF2a	41.36

Table S3.9 Multiple linear regression models showing independent clinical parameters associated with oxidized lipid levels

Clinical parameter	Metabolite	Coefficient	*P* value
CRP	PGF3a	-0.28	0.08
	12-HETE	-0.32	0.06
	16-HDoHE	0.26	0.03
	20-HETE	0.19	0.08
	PGD3	-0.63	0.03
	PGE3	-0.55	0.05
Baseline DAS28	8-iso-PGF2a	0.19	0.06
	14,15-DiHETE	0.26	0.04
	14-HDoHE	-0.39	0.09
	5S,6R-LipoxinA4	0.67	0.01
	NO2-aLA	-0.47	0.02
	NO2-OA	-0.26	0.03
	NO2-LA	-0.48	0.00
DAS28 improvement	PGF3a	0.26	0.02
	PGF2a	0.11	0.02
	iPF2a	0.12	0.02
	NO2-LA	0.18	0.06
	11,12-EpETrE	0.15	0.04
	11-HETE	0.15	0.02
	13-KODE	0.18	0.08
	14,15-DiHETrE	0.10	0.02
	14-HDoHE	0.31	0.03
	15S-HETrE	0.14	0.05
	9-KODE	0.14	0.10
	bicyclo-PGE2	0.14	0.09
	NO2-LA	0.22	0.03

Supplementary Figures

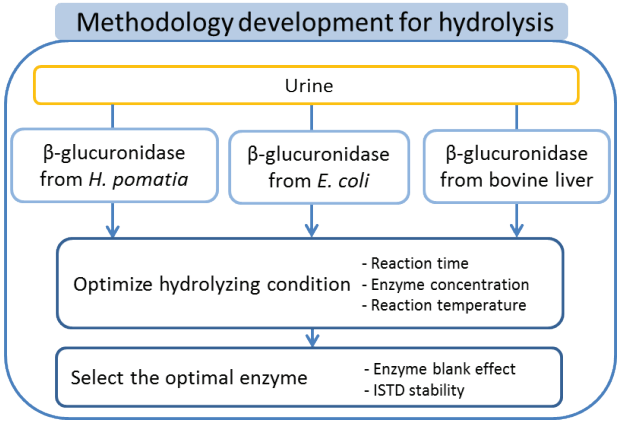

Figure S3.1: Method development overview

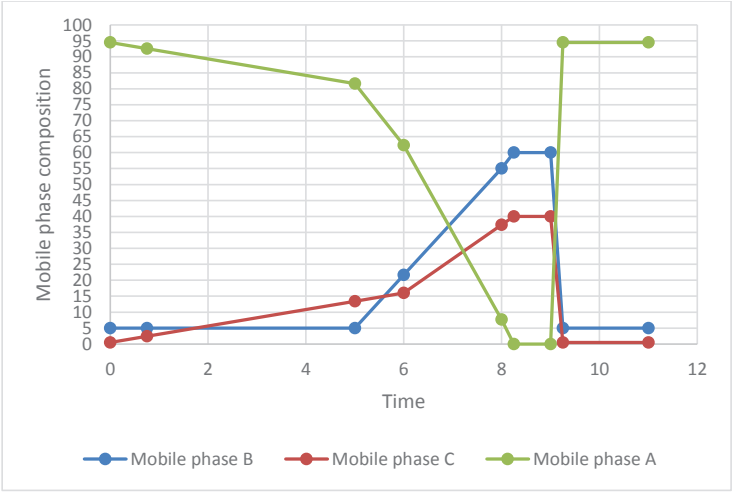

Figure S3.2: Ternary gradient of the used UHPLC-MS/MS method.

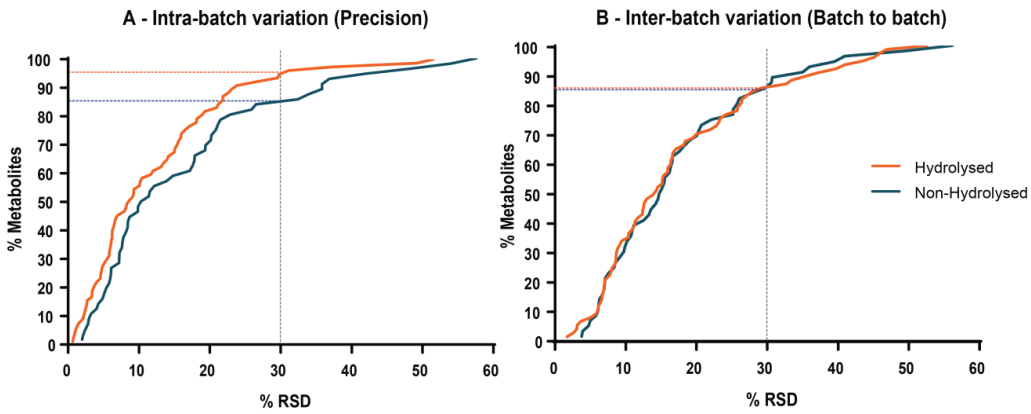

Figure S3.3: Detected endogenous oxidized lipids evaluated for A - precision and B - batch-to-batch effect. More than 90% of endogenous metabolites had an RSD below 30% for the hydrolysed procedure's precision, followed closely with 85% of metabolites in the non-hydrolysed procedure having a precision below 30%. Inter-batch variation indicated similar stable performance across three measurement days for both the hydrolyses and non-hydrolyses procedure.

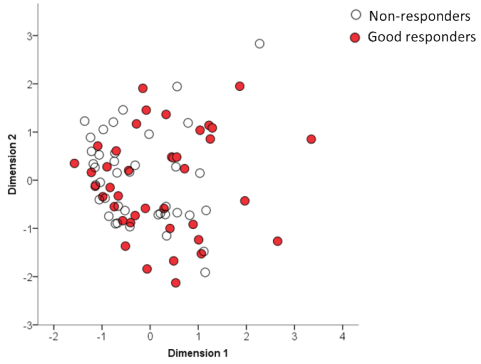

Figure S3.4: Score plot of the CATPCA model for good and non-responders to TNF-α inhibitor treatment of RA patients, depicting component score on Dimension 1 and 2.

3